Bet Hedging in Pdr5-mediated Drug Resistance and a Mechanism for Its Regulation

by

Afnan Azizi

Thesis submitted to the
Faculty of Graduate and Postdoctoral Studies
In partial fulfillment of the requirements
For the M.Sc. degree in
Cellular and Molecular Medicine

Department of Cellular and Molecular Medicine
Faculty of Medicine
University of Ottawa

Abstract

Human health is increasingly threatened by the emergence of multiply drug resistant malignant organisms. Yet, our understanding of the numerous ways by which such resistance arises is modest. Here we present evidence of a bet hedging strategy in the budding yeast, *Saccharomyces cerevisiae*, to counter the effects of cytotoxic drugs through the action of Pdr5, an ATP-binding cassette transporter. We have employed flow cytometry and fluorescent activated cell sorting to probe the expression levels of a GFP-tagged version of *PDR5* in individual cells. The results obtained from these experiments demonstrate that each yeast population is variable in the levels of Pdr5 production, and a small subpopulation of cells produces this efflux pump at much higher quantities than the population average. Consequently, cells with high and low levels of Pdr5 grow differentially in presence and absence of cycloheximide, a cytotoxic drug. These properties are highly suggestive of a bet hedging strategy mediated by Pdr5 levels. We further link this bet hedging strategy to the transcriptional regulatory network of *PDR5* consisting of two major transcription factors, Pdr1 and Pdr3. Our analysis suggests that a self-activating feedback loop acting on Pdr3 plays an important role in generation of the aforementioned subpopulation. Furthermore, our results point to a large difference in the activity of these two regulators wherein Pdr3 is notably stronger than Pdr1. The disparity in their activity could indicate a mechanism for generation of the observed proportions of subpopulations with regards to the level of Pdr5.

Acknowledgements

My utmost appreciation goes to Dr. Mads Kærn whose unceasing mentorship has shaped my scientific career. I am grateful for his support and belief in me, from my first missteps as an untrained undergraduate through to this day.

I would also like to extend my thanks to the members of University of Ottawa's iGEM team, without whom I would not have realized my full potential and achieved what I have most sought.

I am, indeed, indebted to Mila Tepliakova and her patience in teaching me much of what I know about working in a laboratory. I have cherished our many talks.

Anyone would be fortunate to have Hilary Phenix, Ian Roney, and Daniel Charlebois as their colleagues; I thank them for their kind help, our many insightful discussions, and our linguistic debates.

My gratitude goes to Alexander Power and Daniel Jedrysiak for teaching me my first lessons in molecular and synthetic biology and the well trod route to Tim Hortons. I also owe much of my yeasty knowledge to them.

Last, but far from least, I am most grateful to Darija Muharemagic for her friendship and steadfast support in all my endeavours, and to Ana Gargaun for her kindness and concern for my well-being.

Dedication

To all the young people of Ahwaz, who share my ambitions, but have not the fortune to pursue them.

Table of Contents

List of Tables

List of Figures

Chapter 1

Introduction

1.1 Drug Resistance

Rapid advancements in health care and drug-based treatment of maladies, in the past century, have led to an equally swift increase in the emergence of pathogens that can resist these drugs. In fact, the rate at which microorganisms become resistant to newly developed drugs outstrips the rate of their development [1]. Most drugs against microorganisms lose their potency shortly after market introduction as a result of inherent or acquired drug resistance [2], as seen in Figure 1.1. Single cell organisms are not the only malignant living things for which drug resistance has become an alarming problem. Many cancer cells can acquire resistance to chemotherapeutics and become the seeds of metastatic tumours.

1.1.1 Avenues of Drug Resistance

Drug resistance is a stable phenotype wherein an organism can thrive and proliferate in the presence of otherwise inhibiting levels of a drug. It is an evolutionary phenomenon which arises from natural selection of individuals that can negate the effects of the drug in one of several ways. However, cells use two general strategies to overcome the effects of a drug—

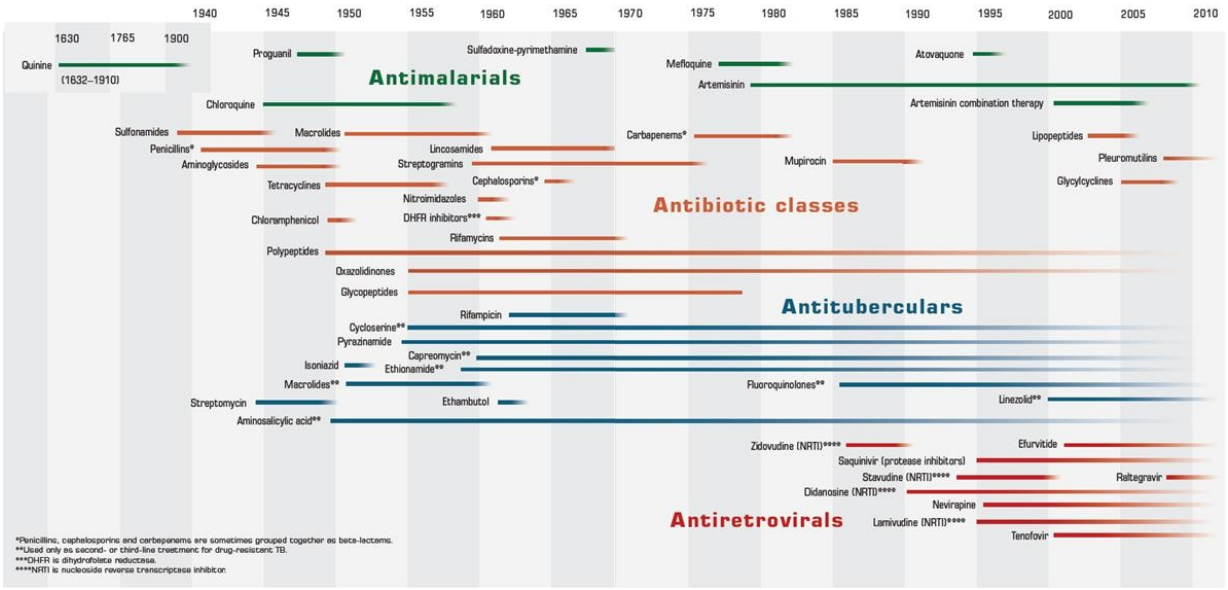

Figure 1.1: The approximate lifetime of antimicrobial drugs after market introduction. Most classes of drugs have a short market life before their target organisms develop resistance to them. Figure reproduced with permission from the Center for Global Development: The Race Against Drug Resistance, copyright 2010.

removal of the drug or its target [3, 4]. Removal of a drug can be manifested in a number of ways, such as its active expulsion from the cell, its enzymatic inactivation, prevention of its entrance to the cell, or its sequestration once it has entered. Similarly, the target may be removed by its mutation, down-regulation, or repair. Mutation or down-regulation of a target is not the most optimal solution for an organism because the drug target is usually essential for its survival. Nonetheless, mutations that alter the structure of the target do occur frequently and decrease effects of the drug. Such mutations often lower the fitness of the organism, at least in the short term, by disturbing the target's function (e.g. see [5]). If a reasonable balance between resistance and lower fitness is struck, the mutant can live long enough to acquire other favourable mutations or conditions that offset the impact of the original mutation [6].

The target itself can remain unchanged if effects of the drug are nullified by other factors. The anti-drug action of these factors can arise as a result of mutations—permanently

changing their functions—or a transient alteration in their state, such as up- or down-regulation [7], post-translational modification [8], or network rearrangements [9], among others. Apart from individuals that possess a mutator phenotype, the rate of random mutations for the majority of the population, under normal conditions, is often quite low—approximately 0.003 per effective genome per division [10]. Many of these mutations are deleterious or neutral, further decreasing the rate of occurrence of beneficial ones. Therefore, in spite of higher mutation rates during stress conditions, including drug treatment, in both microbes [11,12] and eukaryotes [13], the frequency of mutations that would impart drug resistance may not be high enough to account for its prevalence. Hence, mutation-independent mechanisms of variability in a population are likely to contribute significantly to drug resistance and cannot be overlooked.

1.1.2 Heterogeneity and Drug Resistance

Since the initial discovery of antibiotic resistance in bacteria—occurring very shortly after mass market introduction of the first antibiotic—the search for its causes has been ardently pursued. Classically, mutation has been the only known mechanism for the generation of enduring heterogeneity in a population. Naturally, given its role in selection, mutation has been considered to be the major player in acquired drug resistance [14,15]. However, prevalence of drug resistance and the relatively fewer mutations, especially in higher eukaryotes, have led some investigators to re-examine the significance of non-mutational mechanisms in generation of heterogeneity and their implications for drug resistance [9,16–22]. Indeed, non-genetic heterogeneity—i.e. cell-cell variations that are not permanently established by mutations—is abundantly present in all genetically identical populations, and the effects of this kind of heterogeneity on the population are more immediate than those caused by mutations. Furthermore, each cell has the potential to move through all possible biochemical states. Therefore, cells will not have to permanently remain in a state of lower fitness when the environmental conditions change. Because of these properties, this form

of heterogeneity has the capacity to facilitate drug resistance.

The best studied mechanism of transient variability is the noisy expression of genes. In this context, gene expression refers to transcription, translation, and the intervening steps leading to synthesis of functional proteins. All these steps, from the initial binding of transcription factors (TFs) to the final degradation of the protein product of a gene, are biochemical reactions characterized by random diffusion and collision of Brownian particles [23]. Therefore, gene expression is inherently stochastic. The simple gene expression model of Figure 1.2A demonstrates the main biochemical reactions involved in this process. Each reaction is characterized by a rate constant, which is a measure of the average speed of the reaction. However, random fluctuations influence the rate of each chemical reaction, and the strength of their influence depends on the number of starting molecules, volume of the system, and the magnitude of each rate constant [24]. In particular, biochemical reactions which facilitate gene expression usually involve a small number of molecules (e.g. TFs) and are strongly influenced by random fluctuations in the concentration of these molecules. The stochastic nature of these reactions gives rise to bursts of RNA transcription [25], which propagate to cause large fluctuations in the level of resulting protein products (Figure 1.2B). Furthermore, when the gene product is a part of a genetic circuit, noise in its expression will be transmitted to other elements of the same circuit, resulting in correlated fluctuations in their levels [26, 27]. If fluctuations from one state to another are circumstantially slow, these states can be inherited and thus act as substrates for Darwinian evolution. Consequently, non-genetic heterogeneity plays an important role in the stress response of most organisms [28–30].

The presence of a toxic compound in the environment produces a clear stress condition for a cell. Therefore, it is reasonable to expect that mechanisms involved in the biological stress responses would also be involved in drug resistance [31]. Accordingly, non-genetic heterogeneity has gained significant attention in the past decade as an important basis for acquisition of drug resistance. Some of the strongest evidence in support of its role in this

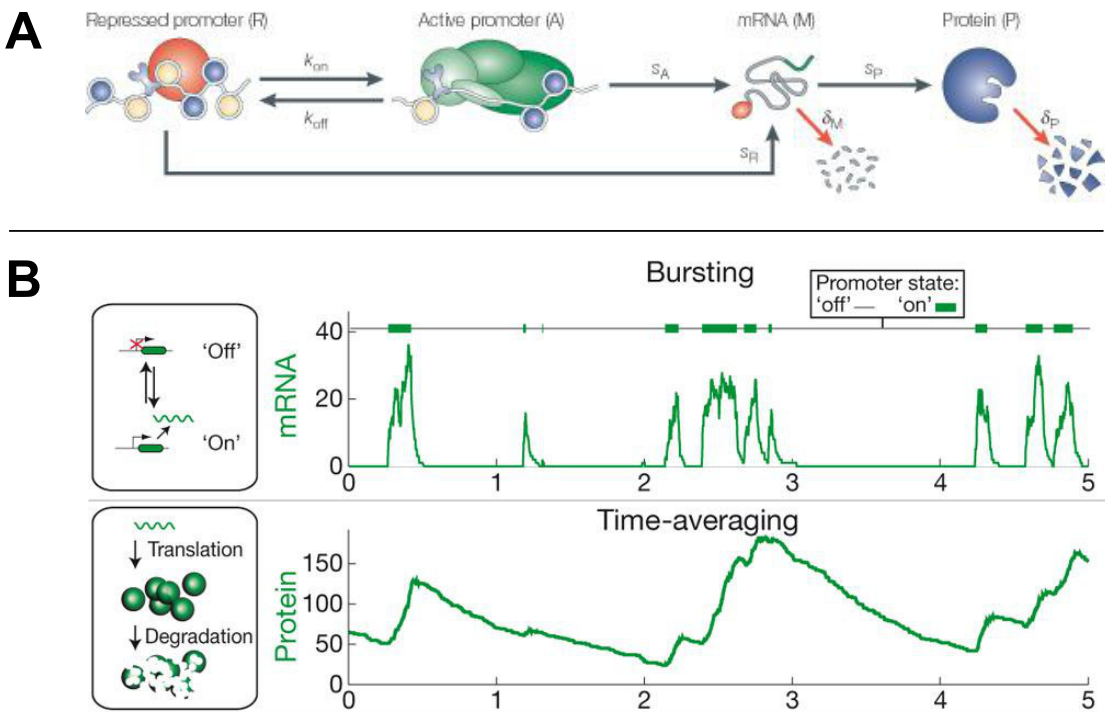

Figure 1.2: Stochastic gene expression. A) A simple model of transcription and translation based on two states of a promoter. In this model each step of the process is a chemical reaction that is characterized by an appropriate rate constant. Reprinted with permission from Macmillan Publishers Ltd: Nature Reviews Genetics 6:451-464, copyright 2005. B) Transcriptional bursting causes large fluctuations in the level of proteins in a biological system over time. Reprinted with permission from Macmillan Publishers Ltd: Nature 467:167-173, copyright 2010.

process come from the field of synthetic biology.

The benefits of studying synthetic systems over natural ones are twofold. First, most synthetic systems are semi-orthogonal to that of the host—i.e. synthetic elements are derived from other organisms and do not interact with the host's genetic networks. Second, these systems are built from well-studied, modular components, facilitating easier and more predictable manipulations. Blake et al. [32] and later Nevozhay et al. [33] used synthetic networks and exogenous drug resistance genes in *Saccharomyces cerevisiae* for this purpose. Both of these groups demonstrated that larger variability among individual cells in a population—due to noisy promoter dynamics or stochastically-induced bistability, respectively—leads to a better chance of survival and a higher population fitness in response to prohibitive levels of drug.

These results are not limited to synthetic systems. *Escherichia coli*, as well as other bacteria, can become dormant—i.e. have a growth rate of nearly zero—and escape the effects of antibiotics. Entrance into dormancy, in *E. coli*, has been shown to rely on the level of an endogenously produced toxin [34]. This toxin can only act when it is present above a certain threshold, which is randomly crossed by a small subpopulation of cells [22]. In cancer cells, too, the contribution of non-genetic heterogeneity to drug resistance has been reported. Levchenko et al. [35] reported the intercellular transfer of P-glycoprotein (P-gp), a *Homo sapiens* membrane drug pump, and acquisition of drug resistance by previously drug-sensitive cells. Generation and propagation of such drug resistant pockets within tumours result in a genetically identical, but phenotypically variable, population that can survive treatment. In fact, it has been known for many years that P-gp and some anti-apoptotic pathways are regulated by a network architecture [36] that could increase stochastically-induced variability [27]. More directly, researchers have performed single-cell proteomics analyses of approximately 1000 proteins in cancer cells under drug treatment [37]. They have found that, while cells showed normal levels of variability in protein levels before treatment, the addition of the drug amplified this variability within

a small subset of proteins. Finally, they demonstrated that cells with higher levels of one of these variably-produced proteins have a better chance of surviving drug treatment than those with lower levels.

This accumulating body of evidence has led Brock et al. [18] to offer a fresh view on the issue of cancer phenotype emergence and maintenance. They suggest that phenotypic variability of genotypically identical cells is a potential mechanism of drug resistance in cancer cells. They argue the following: because mammalian cells do not mutate quickly, natural selection is more likely to occur on phenotypic variants than genotypic ones. Suppose that levels of a protein that modulates survival of cancer cells during drug treatment are variable within the tumour population. A subpopulation with higher levels of this protein would undergo Darwinian selection if it can maintain these levels over at least one generation. Furthermore, since most anti-cancer drugs cause DNA damage, the surviving population is more likely to develop lasting, favourable mutations and acquire permanent resistance [18, 21]. Recently, two studies have provided tangible results in support of this role of heterogeneity in drug response. Sharma et al. [9] identified a small subpopulation of a cancerous cell line with reversible drug tolerance that appears to be controlled through chromatin dynamics. Additionally, Kreso et al. [17] have functionally correlated variability in the *in vivo* repopulation kinetics—rate of tumour propagation—among xenografted clonal cancer cells with their ability to resist therapy. The authors found that, within the clonal populations, up to five categories of cells with distinct growth dynamics existed, which could explain their variable response to the drug.

In addition to these studies, computational and mathematical models are increasingly used to investigate the possibility of and the requirements for drug resistance in heterogenous populations of isogenic cells. The advantages of stochastic heterogeneity in stress-response mechanisms within randomly changing environments have been extensively modelled since the beginning of the current century [38–41]. Recently, however, researchers have focused on specifically understanding the problem of drug resistance and mathemati-

cally exploring the role of stochasticity in its emergence. For example, modelling has been used to generate diagrams representing 'fitness landscapes', which can capture the fitness of a population over a range of drug concentrations and levels of its cognate resistance gene [19, 33]. A fitness landscape developed for *E. coli* allowed Deris et al. [19] to determine critical concentrations for a drug above which the population became bistable for the expression of the drug resistance gene. These results were confirmed experimentally. Nevozhay et al. [33], on the other hand, found that the expression of an exogenous drug resistance gene in *S. cerevisiae* is taxing to the organism at high levels. The fitness landscape, in this case, showed a clear 'sweet spot' level of expression for the drug resistance gene that would maximize the organism's fitness. Furthermore, analysis of experimental data regarding the ability of two breast cancer cell lines to populate three distinct phenotypic states in absence or presence of a drug, led Gupta and colleagues [42] to develop a quantitative model to describe state switching among these cells. The authors calculated the probabilities of switching from one state to another, along with cell viability in each state, and accurately simulated the population composition after drug treatment. Finally, Charlebois et al. [43] have shown, performing *in silico* simulations of cell populations, that noisy gene expression, coupled with some stability in the level of a drug resistance factor, is sufficient to make a subset of the population permanently resistant to a drug. For this scenario to work, the levels of the drug resistance factor in the population must be variable, and the cells with high levels have to maintain them until the first cell division. Under these conditions, cells with low levels will perish, and the population will consist only of the high expressing cells, effectively increasing the population mean level of the drug resistance factor (Figure 1.3).

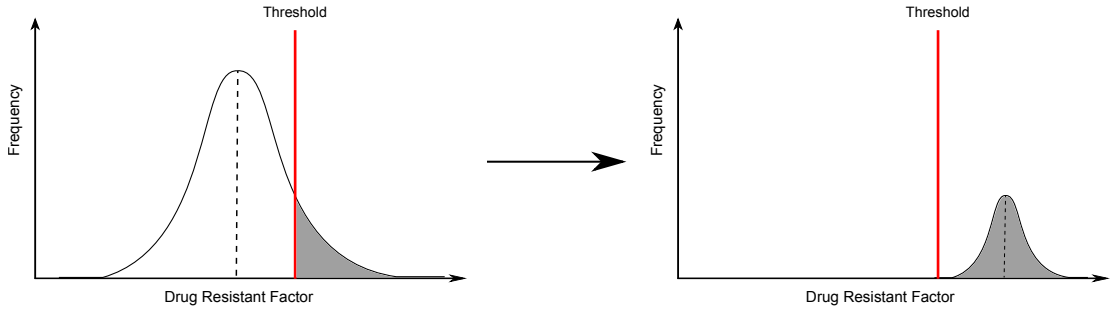

Figure 1.3: Establishment of drug resistant populations independent of mutations. When a population is exposed to a certain amount of a drug that would kill all cells below a threshold, those with a higher level of a drug resistance factor would survive the initial drug treatment. However, they can only survive and establish a high-level population if they can maintain this level for more than one generation.

1.2 Heterogeneity—Bet Hedging

The concept of bet hedging as an evolutionary phenomenon was conceived more than 40 years ago [44–46]. As the name implies, this strategy had been previously investigated and used extensively in economics and finance to minimize the risk of uncertain ventures. To give an example, if one were to repeatedly bet one's entire earnings on the horse with the best odds of winning in a horse race, one would maximize one's performance in the majority of the times. However, when that horse loses, all of one's earnings are lost, and one is eliminated from the competition. Therefore, it is beneficial to hedge one's bets and lose some of the profit in each race in order to avoid complete elimination in case of unfavourable outcomes. This strategy is only practical when the advantage gained by avoiding the deleterious effects of unfavourable conditions far exceeds the disadvantage caused by lower profits during favourable conditions.

Formally, in bet hedging, a given genotype is optimal when it has a larger geometric mean fitness over time than others, even if its arithmetic mean fitness is smaller. In temporally stable environments where the fitness of a given genotype remains constant over time, the geometric and arithmetic fitness means are identical. However, because the multiplicative nature of reproduction directly governs fitness, the geometric mean provides a

better measure for it than the arithmetic one in a changing environment [47]. Furthermore, the genotype that maximizes geometric mean fitness does so by minimizing the variance in fitness over time, which is evolutionarily favourable [45, 48, 49].

Originally, bet hedging was used to describe the incidence of smaller than possible clutch sizes. In this tactic, the organism sacrifices the benefit of maximum fecundity in order to offset the prohibitive cost of placing all its resources in reproducing and maintaining a large clutch that may be completely destroyed by unpredictably changing environmental conditions [50]. This form of bet hedging is termed *conservative* [51]. Mountford [52], on the other hand, used the idea of *diversified* bet hedging, while not branding it as such, to explain why some populations would maintain non-breeding adults. He demonstrated that, in the face of extreme conditions, the more resilient non-breeders form a reserve to reestablish the population, which increases its long-term growth rate. This latter use of bet hedging to explain evolutionary phenomena did not gain much attention at the time [38, 53], possibly due to an inability to experimentally study and manipulate bet-hedging populations.

The definition of bet hedging, however, has evolved and been much debated since its initial use. In the context of this work, bet hedging is primarily a risk spreading strategy. This strategy occurs when a population can reversibly diversify its phenotype, whereby one or more distinct phenotypes are disadvantageous in normal conditions, but have an increased fitness under extremely unfavourable ones. Therefore, when the probability of occurrence of such conditions is non-zero and the environment randomly switches between them, decreasing the detrimental effects of the extreme ones can be more favourable than maximizing the fitness during the normal one [54–61]. It is worthy to note that merely possessing variable phenotypes does not demonstrate the presence of a bet hedging strategy; these phenotypes must differentially affect the fitness of an individual under distinct conditions [54].

A large body of mathematical modelling and computational simulations has been pro-

duced in an attempt to describe the properties of bet hedging and to derive the optimal strategies for different kinds of organisms, populations, or environments [38,40,55,59,60,62, 63]. On an experimental level, however, much work remains to be done in order to demonstrate the significance of bet hedging as a survival strategy, especially in eukaryotes [64]. One of the first examples of bet hedging was found in *E. coli* where a complex network of regulatory factors, including DNA methylation, gives rise to phases of ON and OFF fimbrial fibre production [65]. While fimbrial fibres are required for initial host colonization by bacteria, their production is both metabolically expensive [65] and is correlated with higher chances of phagocytosis by the host leukocytes [66], signifying this as a bet hedging strategy. Since then, the use of bet hedging by more than one family of bacteria—e.g. enterobacteria and mycobacteria—to maintain a small population of persister cells has been documented [22, 67]. In *Bacillus subtilis*, a subpopulation of cells was shown to undergo epigenetically-driven sporulation under metabolic stress, thereby preparing a portion of the population for long term survival if the conditions were to further deteriorate [68]. Indeed, Beaumont et al. [58] directly observed the evolution of bet hedging in the bacterium *Pseudomonas fluorescens* through causative mutations that allowed the population to maintain a heterogenous phenotype able to survive sequential switching between two opposing environmental conditions.

The experimental evidence for bet hedging in higher eukaryotes is presently controversial. Effects similar to those seen in *P. fluorescens* have been observed in *S. cerevisiae*, but only in a man-made synthetic system [69]. In this case, two strains were designed to stochastically switch between two expression states—low and high. One switched slowly while the other did so rapidly. Then, each strain was subjected to sequential growth in two opposing environments; one imparted higher fitness to the low expressing subpopulation and the other to the high expressing subpopulation. It was demonstrated that the strain with slow switching rate had a higher fitness when the rate of environmental change was small, while the other survived better in rapidly switching environments. These

results agree well with findings that, for large populations, the proportion of cells possessing the lower-fitness phenotype is correlated with the frequency of the occurrence of the unfavourable condition [60, 70, 71].

It has recently been suggested that some prions enhance survival under environmental stress and are, thus, nominated as likely agents for bet hedging in yeast [56]. In addition, Levy et al. [72] have observed the first potential case of naturally occurring bet hedging in *S. cerevisiae* and identified the gene by which it is mediated. They show that the higher expression of *TSL1*—a gene involved in trehalose biosynthesis—is correlated with lower growth rates, as well as improved response to heat shock. However, they observe that Tsl1 accumulates preferentially in aging cells, which confounds the role of Tsl1 in causing the observed growth rate differences. Therefore, despite these efforts, conclusive proof of bet hedging, as a naturally occurring mechanism to cope with environmental fluctuations, is lacking in eukaryotes.

1.3 Heterogeneity—Network Architecture

The regulatory networks that control gene expression play crucial roles in defining the properties of non-genetic population heterogeneity. These networks generally enhance the information processing capacity of the genome by expanding the number of possible outputs that can be derived from the same inputs. The structure and connectivity—also known as architecture or topology—of a network, like the formula of a mathematical function, specify the types and properties of the outputs it generates. Therefore, since different network architectures can yield diverse outputs, they become substrates for natural selection and some are maintained throughout evolution of an organism's genome. Physical and regulatory interactions can come about accidentally due to random mutations. However, whether these interactions are maintained is determined by their benefit—or harm—to the organism. Research has established that large interconnected genetic networks can often be

reduced to recurring patterns of interactions that contain few genes [73]. These patterns, or network motifs, have distinct properties and exist in proportions that are higher than would be expected due to randomly occurring interactions [74, 75]. Of these, the feedforward loop (FFL) motif and the feedback loop (FBL) motif are two of the most biologically common ones that are found in nearly all organisms [73, 76].

1.3.1 Feedforward Loop Motif

This network motif consists of three nodes—i.e. genes—and three edges—i.e. regulatory interactions. One gene, X, regulates the expression of two others, Y and Z, while Y only regulates that of Z. Depending on the regulatory sign of each of the three interactions—negative for inhibition and positive for activation—eight distinct FFL subtypes can be produced, as outlined in the top panel of Figure 1.4. The subtypes can be grouped under two categories based on the overall sign of the direct and indirect regulatory routes—i.e. $X \longrightarrow Z$ and $X \longrightarrow Y \longrightarrow Z$. If both have the same overall sign, the FFL is coherent; otherwise, it is incoherent. This motif can be further diversified based on the combinatorial logic of the regulatory interactions acting upon Z. If both X and Y are required for the expression of Z, an AND gate is formed; if only one is sufficient, it gives rise to an OR logic gate [77].

Type-I coherent and type-I incoherent FFLs (C1FFL and I1FFL, respectively) are the most frequently occurring FFLs in nature [78, 79], but have very different regulatory dynamics from one another. For instance, C1FFL causes a delay in the response of the network to an external stimulatory signal, depending on its output logic. If it is an AND gate, then the delay manifests upon addition of the signal—the ON step—because of the lag time between induction of X and sufficient accumulation of Y. By the same token, the lag time between termination of X induction and dissipation of Y leads to a delay upon removal of the signal—the OFF step—in the OR gated C1FFL [80].

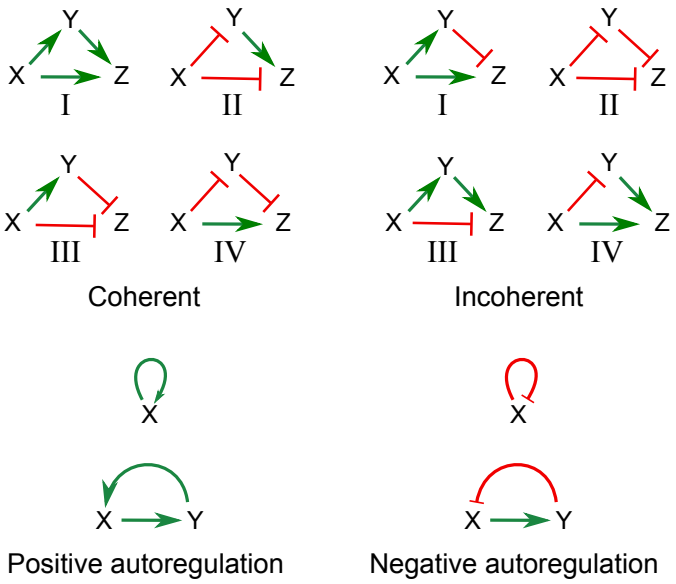

Figure 1.4: The various possible configurations of feedforward loop and feedback loop motifs. The eight possible permutations of a feedforward loop are depicted in the top panel. If the overall sign in both the direct and indirect routes of regulation are the same, the motif is coherent, otherwize it is incoherent. The subtypes were arbitrarily assigned by Mangan et al. [77]. The bottom panel shows self-activatory (left) and self-inhibitory (right) configurations of the feedback loop motif either with one (top) or two (bottom) nodes.

In contrast, I1FFL accelerates the response to signals at the ON step under the AND logic—OR logic is not defined for this category of FFLs. Response acceleration stems from the inhibitory action of Y and is in comparison to a scenario where Z is directly activated by X. In order for Z to reach the same steady-state level in both scenarios, X needs to overshoot Z activation to counteract the ensuing inhibitory action of Y [77, 79]. This phenomenon is, in fact, used in natural and synthetic networks for pulse generation and fold change detection [80–82].

Most interesting is the ability of FFLs to process input noise differentially based on their architecture. For example, Kittisopikul and Süel [83] demonstrated that for the FFL subtypes in which the $X \longrightarrow Y$ edge is activating—including both C1FFL and I1FFL—expression of Z is much more bursty than when it is an inhibitory edge. Therefore, these subtypes promote stochastic initiation of Z expression and, in *E. coli*, are mainly enriched in functional categories involved in rare processes, such as stress response [83]. It was further shown by Swain and colleagues that the C1FFL regulatory network is generally associated with higher variability in gene expression than I1FFL [84]. This outcome is because of an increase in noise through two activating routes—constructive interference—of C1FFL unlike its reduction due to the opposing inhibitory route—destructive interference—in I1FFL.

1.3.2 Feedback Loop Motif

All self-regulating complex systems must use information feedback to permit modulation of an input by its output [85]. Therefore, it is not surprising to find single, double, and multi-node FBLs, in abundance, in all living systems. Regardless of their number of nodes, FBLs are either positive or negative (Figure 1.4, bottom panel) depending on whether the output amplifies or suppresses its own production, respectively. In genetic networks, negative and positive FBLs have diverse properties and functions. In the case of a negative FBL, it

decreases response times to a given signal compared to a simple activation network with the same steady-state level [75, 86]. In addition, it limits expression deviations from that steady-state level. Therefore, negative FBLs attenuate noise and stabilize the level of a product in both natural and synthetic networks [24, 87–90].

Positive FBLs, however, function in the opposite manner. In fact, this motif fosters variability by amplifying small deviations [24, 91]. Furthermore, positive FBLs can perpetuate their own expression and, thus, persist for long periods of time resulting in 'expression memory'. Combining these two main features of positive FBLs, a population can have two distinct expression states which are stable over time. This bistability is attained due to the complementary positive-FBL effects of noise amplification to achieve high expression and memory of the expression state caused by its perpetuity [27, 76, 92–94]. Interestingly, bistability can be avoided, in favour of bimodality, if the active form of the TF is made unstable to enhance stochastic restoration of the non-expressing state [29, 95].

1.4 Pleiotropic Drug Resistance

In the biological warfare against microbes and cancers, the only thing that is more threatening than drug resistance is multiple (pleiotropic) drug resistance (MDR/PDR). As malicious cells become resistant to traditional drugs, the use of newer and stronger cytotoxic agents increases. In addition, many pathogens need to be treated with drug cocktails to ensure their complete removal [96]. These treatment regimens place a great selective pressure on populations of organisms to evolve MDR. In bacteria, and other pathogenic microbes, MDR is often acquired by consecutive mutations and/or horizontal gene transfers. Additionally, MDR can be acquired through the action of transmembrane pumps that actively expunge diverse classes of drugs from cells [97]. In fact, the use of transmembrane efflux pumps is the major avenue of MDR in mammalian cells and other higher eukaryotes [98]. Transmembrane drug efflux pumps are often able to recognize and expel tens

of structurally or functionally unrelated compounds from the cell. Five major superfamilies of multidrug transporters are in existence across all domains of life—major facilitator superfamily (MFS), ATP-binding cassette (ABC), multidrug and toxic compound extrusion (MATE), resistance nodulation division (RND), and small multidrug resistance (SMR) transporters [99]. Among these, members of the first two superfamilies are most implicated in eukaryotic MDR from fungal pathogens to cancer cells [98, 100, 101].

As the largest family of secondary active transporters with more than 10,000 sequenced proteins across all kingdoms [102], MFS members function as uniporters, symporters, and antiporters. These transporters are crucial for the survival of cells and partake in such activities as glucose uptake—e.g. GLUT1 of *H. sapiens*—transport of amino acids and other metabolites—e.g. Hip1 of *S. cerevisiae*—phosphate:organophosphate exchangers—e.g. Pho-5 of *Neurospora crassa*—as well as drug efflux. The drug clearance is typically carried out by drug:H^+ antiporters [103, 104].

The ABC transporters are the other important superfamily of membrane pumps. They derive the energy for active transport of various substrates across membranes by hydrolyzing ATP—a feature which has been conserved among all studied organisms. ABC transporters serve as either importers—in prokaryotes—or exporters—in prokaryotes and eukaryotes—of ions, amino acids, oligopeptides, sugars, lipids, and other hydrophobic compounds [105]. Several ABC transporters act to clear hydrophobic, aromatic, and other small organic compounds and have the ability to generate MDR. Of these transporters, the *H. sapiens* P-gp is by the far the most extensively studied, and its role in intrinsic and acquired MDR of numerous cancer cell lines has been elucidated. On one hand, tissues with naturally high expression of P-gp are more prone to give rise to intrinsically drug resistant tumours [106]. On the other hand, a high level of P-gp has been shown to take part in MDR acquisition of other tumour types, such as acute myeloid leukaemia [106, 107]. Interestingly, significant natural, inter-individual variability in the level of P-gp—on both mRNA and protein levels—in the gastrointestinal tract has been widely reported [108, 109]

and is speculated to lead to aberrant drug response in patients.

Among fungal pathogens, *Candida albicans* is the species most commonly responsible for candidiasis, as well as opportunistic pathogenesis in immunosuppressed patients. High expression of Cdr1, the most prevalent ABC transporter of *C. albicans*, in clinical isolates has been associated with decreased susceptibility to the azole class of antifungals (ergosterol biosynthesis inhibitors), cerulenin (a fatty acid biosynthesis inhibitor), and some echinocandins (disruptors of cell wall synthesis), among others [101, 110].

Naturally, the direct study of pathogens and malignant cells could pave the way for rapid translation of experimental results into treatment strategies. However, the complexities of basic, exploratory research in these organisms prompt us to make use of more tractable model organisms. The budding yeast, *S. cerevisiae*, was the first eukaryote whose genome was completely sequenced [111], and has been, undoubtedly, the model organism upon which much of microbiology and medicine has been founded [112]. Given the wealth of knowledge about *S. cerevisiae* and its accessible biology, it is the model of choice in many biological studies. Furthermore, drug resistance pathways have been characterized extensively in *S. cerevisiae*, which deem it a suitable candidate for investigating the emerging concepts of non-genetic drug resistance.

Pleiotropic drug resistance in *S. cerevisiae* is mediated through an interconnected network of TFs and transmembrane pumps, which interact closely with the general stress response and lipid biogenesis pathways of yeast. Twenty known proteins take part in the PDR network, of which six are TFs, nine are ABC transporters, and the rest are metabolic regulators and other interactants [113]. Pdr1 and Pdr3 are the two major transcriptional regulators of PDR and possess binding sites on the promoters of many of the other genes involved, forming a complex network of interactions with cascades, feedback and feedforward motifs (Figure 1.5A). Pdr5, the *S. cerevisiae* homologue of Cdr1 and P-gp, is the most prominent gene among ABC transporters and has been extensively studied for its role in MDR [114].

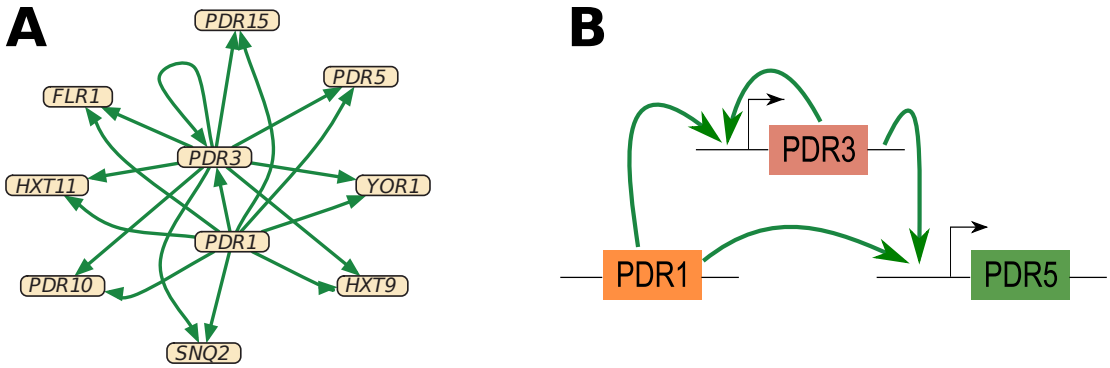

Figure 1.5: The regulatory network of PDR in *S. cerevisiae* and its motifs. A) Regulatory interactions between Pdr1 and Pdr3, the main TFs in PDR, and some of their more prominent targets. Adapted from BioMed Central Ltd: Genome Biology 6:R35, 2005 freely available under the terms of the Creative Commons Attribution License. B) A close-up on the regulatory network architecture of *PDR5*, under the control of Pdr1 and Pdr3, which form a type-I coherenet feedforward loop.

1.4.1 *PDR5*

PDR5 is a 4536 base pair (bp) gene on the q arm of *S. cerevisiae* chromosome XV, coding for a 170 kDa protein of 1511 amino acids (aa). Pdr5 consists of two sets of nucleotide binding domains and transmembrane domains (NBD-TMD) placed in tandem. Both NBDs are highly conserved in all species and contain the signature ABC domains. Each TMD contains six putative α-helices, which span the membrane, and can take one of two conformations. The conformation that creates an inward facing cavity—towards the cytosol—is thought to have a higher affinity for the substrate than the outward facing cavity [113,114]. Binding of two ATP molecules—possibly cooperative—to the NBD-NBD dimer causes a conformational change in the TMDs from the inward facing cavity conformation to the outward facing one, whereby the substrate is transported and released outside the cell. Hydrolysis of ATP to ADP, and its subsequent release, reverses the conformational change and prepares the pump for another transport [105]. Unlike many other ABC transporters, ATP-hydrolysis activity of Pdr5 is not coupled to the amount of substrate present; in fact, it continuously hydrolyzes ATP at a rate of about 28 s^{-1} [114,115], suggesting its role in cellular detoxification from harmful metabolic byproducts [116]. Pdr5 activity has been

correlated to enhanced resistance and survival of *S. cerevisiae* upon encountering tens of compounds from diverse classes. Also, a large promiscuity in substrate selection has been observed among Pdr5 and two other important ABC transporters—Snq2 (Sensitivity to 4-NitroQuinoline-N-oxide) and Yor1 (Yeast Oligomycin Resistance)—which ensures effective MDR in face of a large range of xenobiotics [117–119].

PDR5 was discovered as a non-essential gene whose absence sensitized *S. cerevisiae* cells to both cycloheximide and sulfometuron methyl [120]. Soon after its discovery, it was determined that the promoter of *PDR5* contains multiple binding sites for two previously identified TFs, Pdr1 and Pdr3 [121, 122]. These TFs bind to four binding sites on the promoter of *PDR5* designated Pdr1/Pdr3 response elements—or PDREs. Two perfect PDREs with the sequence 5'-TCCGCGGA-3' are interspersed with two deviating PDREs with the sequence 5'-TCCGTGGA-3'. These PDREs are located in the range of -563 to -304 from the start codon of *PDR5* [123]. Multiple lines of evidence suggest that the sequence spanned by the PDREs forms a nucleosome depleted region, whereas two well-defined nucleosomes reside at the proximal region of the promoter coinciding with the TATA box and transcriptional start site of *PDR5* [124, 125]. Given generally noisy transcription from TATA containing promoters [126] and the evidence for nucleosomal occupancy at that position, bursty mRNA transcription from the *PDR5* promoter [127] is indeed expected. Apart from Pdr1 and Pdr3, another transcriptional regulator modifies the expression of *PDR5*. Rdr1 has been shown to bind to the *PDR5* promoter and acts as a repressor increasing drug sensitivity in the absence of the other TFs [116, 128].

1.4.2 Master Regulators—*PDR1* and *PDR3*

These two major TFs control the expression of many PDR genes, as well as some lipid homeostasis, metabolic, and stress response elements. Pdr3 and Pdr1 belong to the exclusively fungal family of zinc cluster TFs—exemplified by the well-studied Gal4—whose

DNA-binding domains consist of six conserved cysteine residues chelating two zinc ions, Zn_2C_6 [129]. They are paralogous, arising from the yeast whole genome duplication event millions of years ago, and share 36% aa homology [130]. The middle portions of these two TFs—involved in dimerization and regulatory interactions—show a much higher homology than either terminus. In particular, despite having similar sizes, their acidic C-terminal activation domains do not share much sequence identity [131–133]. Nonetheless, both Pdr1 and Pdr3 recognize PDREs, and their regulation of most PDR genes are dependent on these elements [122]. Indeed, they can bind PDREs as homo or heterodimers, thereby increasing the combinatorial variety of PDR transcriptional regulation [129,134]. Delahodde et al. [135] identified two PDREs in the promoter of *PDR3*, establishing the role of Pdr1 in activating the expression of this TF and demonstrating the presence of an autocatalytic positive FBL. This set-up of the regulatory network modulating the expression of *PDR5* constitutes a C1FFL, which arises from the concurrent activation of *PDR5* and *PDR3* by Pdr1, along with the activation of *PDR5* by Pdr3 (Figure 1.5B).

A consensus about the exact mechanism of *PDR5* regulation by Pdr1 and Pdr3 is yet to be reached. Chromatin immunoprecipitation evidence suggest that Pdr1 is present on the promoter of *PDR5*, as well as other PDRE-containing promoters, even without drug treatment [136]. This observation is consistent with a significant steady state expression of Pdr5 in cells growing with fermentable carbon sources [116], and a rapid increase in transcription of *PDR5*—within five minutes—upon drug treatment [125]. High-throughput analysis of GFP-tagged protein levels in rich media at steady-state has given an indication of the relative amounts of Pdr1 and Pdr3. According to these studies, the number of Pdr5 proteins are in the tens of thousands, while those of Pdr1 and Pdr3 are in the thousands and hundreds, respectively [137]. These values are consistent with a model where *PDR5* is activated by a constitutively promoter-resident Pdr1, whose activity increases after binding to drug substrates.

Nonetheless, some discrepancies remain regarding regulation of *PDR1* and *PDR3* on

one hand, and their control of *PDR5* on the other. One group of researchers supports a nuclear receptor-like model for the activation of Pdr1 and Pdr3, backed by radiolabelled ligand displacement experiments for some drugs, including cycloheximide, and enhanced co-immunipercipitation of general transcriptional activators—e.g. members of SAGA and Mediator complexes—with drug-bound Pdr1 [138, 139]. Yet, others maintain that neither Pdr1 DNA binding nor its recruitment of these activators is modified by its association with drugs [124, 136]. The uncertainty in a comprehensive understanding of Pdr1/Pdr3 regulatory mechanisms is further exacerbated by a number of observations. First, the identification of a binding site for Rpn4 in the promoter of *PDR1* [140] and functional activation of *PDR1* by this TF [141] have been the first demonstration of a transcriptional regulator of *PDR1*, but have remained largely unexplored. Rpn4 is a zinc finger transcription factor which upregulates most of the proteasome genes in *S. cerevisiae*, and is in turn activated by a variety of stress conditions. Hence, given that *RPN4* is regulated by both Pdr1 and Pdr3 [142, 143], a multicomponent positive feedback among these three transcription factors exists, at least under certain conditions. Second, it has been long discovered that Pdr3 becomes active upon mitochondrial genome loss, resulting in high Pdr5 expression and drug-independent drug resistance, in ρ^0 yeast cells [144, 145], but the mechanism of such activation has remained unresolved.

1.5 Hypotheses

1. The cell-cell variability in the level of the *PDR5* gene product improves survival in presence of drugs and highlights a bet hedging strategy in *S. cerevisiae* drug resistance.

2. The architecture of the transcriptional regulatory network, controlling *PDR5* expression, enhances cell-cell variability in its levels.

1.6 Specific Aims

1. Characterization of Pdr5 expression profile and its properties in presence and absence of drug.

   (a) Tagging of Pdr5 with yeast-enhanced green fluorescent protein (yEGFP) and characterization of the cell population based on the Pdr5-yEGFP expression profile.

   (b) Investigating the properties of the different subpopulations before and after drug treatment using flow cytometry and cell sorting.

2. Probing the role of each TF, as well as the network structure, in regulating the expression of *PDR5* and response to drug treatment.

   (a) Generation and study of mutants lacking either *PDR1* or *PDR3* to investigate activation of *PDR5* by only the positive FBL of Pdr3 or direct activation by Pdr1, respectively.

   (b) Generation and study of mutants containing one copy of *PDR1* or *PDR3* regulated by the other factor's promoter to study the same network motifs as in 2(a), but comparing the activities of the two TFs.

Chapter 2

Materials and Methods

2.1 Construction of Parts

The various DNA constructs, to be transformed in yeast cells, were constructed using overlap extension polymerase chain reaction (PCR). Each individual DNA sequence—comprising one part—was amplified from isolated genomic DNA or plasmid DNA, using a forward primer (FP) that contained some homology for the previous part and a regular reverse primer (RP). The area of homology, added as an overhang onto FP, was the reverse complement of the previous part's RP; thus, matching its thermodynamic properties. Individual parts—or monomers—were amplified using a conventional PCR program. Target genomic or plasmid DNA was denatured at 98°C for 5 or 2 min, respectively. Primers were allowed to anneal for 20 s at a temperature calculated to be the average of the melting temperatures of FP and RP. Extension was carried out at 72°C, and its time was based on the length of the part to be amplified; it was calculated to correspond to 15 s for every 1000 bp. Each amplification was repeated for 25-30 cycles depending on previously observed efficiency and the amount of final product required.

These monomers were then used to build dimers, trimers, or tetramers. The desired number of monomers were mixed at roughly equimolar concentrations; this was achieved

by adding 50 ng of each monomer per 1000 bp of its length. All required reagents for PCR were added except primers, and the monomers were pre-cycled for at least 13 cycles. The annealing temperature was based on the average melting temperatures of all relevant areas of homology. Extension time was set to correspond to the longest part. Following the pre-cycling, FP of the first part and RP of the last part (end primers) were added to the mixture, and another round of at least 12 cycles was performed. At this stage, the annealing temperatures were changed to the average melting temperatures of end primers, and the extension time was based on the total length of the expected multimer. See Figure 2.1 for a schematic representation of this process.

Reagents for each PCR reaction were as follows: 1X Phusion HF Reaction Buffer (#B0518S, New England BioLabs), 200 μM deoxynucleotide mixture (#N0447S, New England BioLabs), 10 μM of each primer (Invitrogen and Integrated DNA Technologies), and 1 U of Phusion HF DNA Polymerase (#M0530L, New England BioLabs). A Mastercycler EP Gradient thermal cycler (#D-5002-1001, Eppendorf) was used for all PCR reactions. Success of amplification was confirmed by gel electrophoresis using a 1.5% agarose gel in 1X TAE buffer at 80 V for 30-60 min depending on the size of the amplified part.

2.2 Yeast Cell Manipulations

2.2.1 Transformation

The LiAc/SS carrier DNA/PEG method of Gietz and Schiestl [146] was employed for all yeast transformations. Briefly, an overnight culture of yeast cells was diluted in 2×YPD media to a density of 5×10^6 cells/mL. This culture was placed in a shaking incubator at 200 rpm and 30°C for ∼4 hours until it reached a density of 2×10^7 cells/mL. Cells were centrifuged at 4000 rpm for 5 min, in a durafuge 100 (Precision), and were washed three times with autoclaved deionized water (ddH_2O). For each separate transformation, 1×10^8

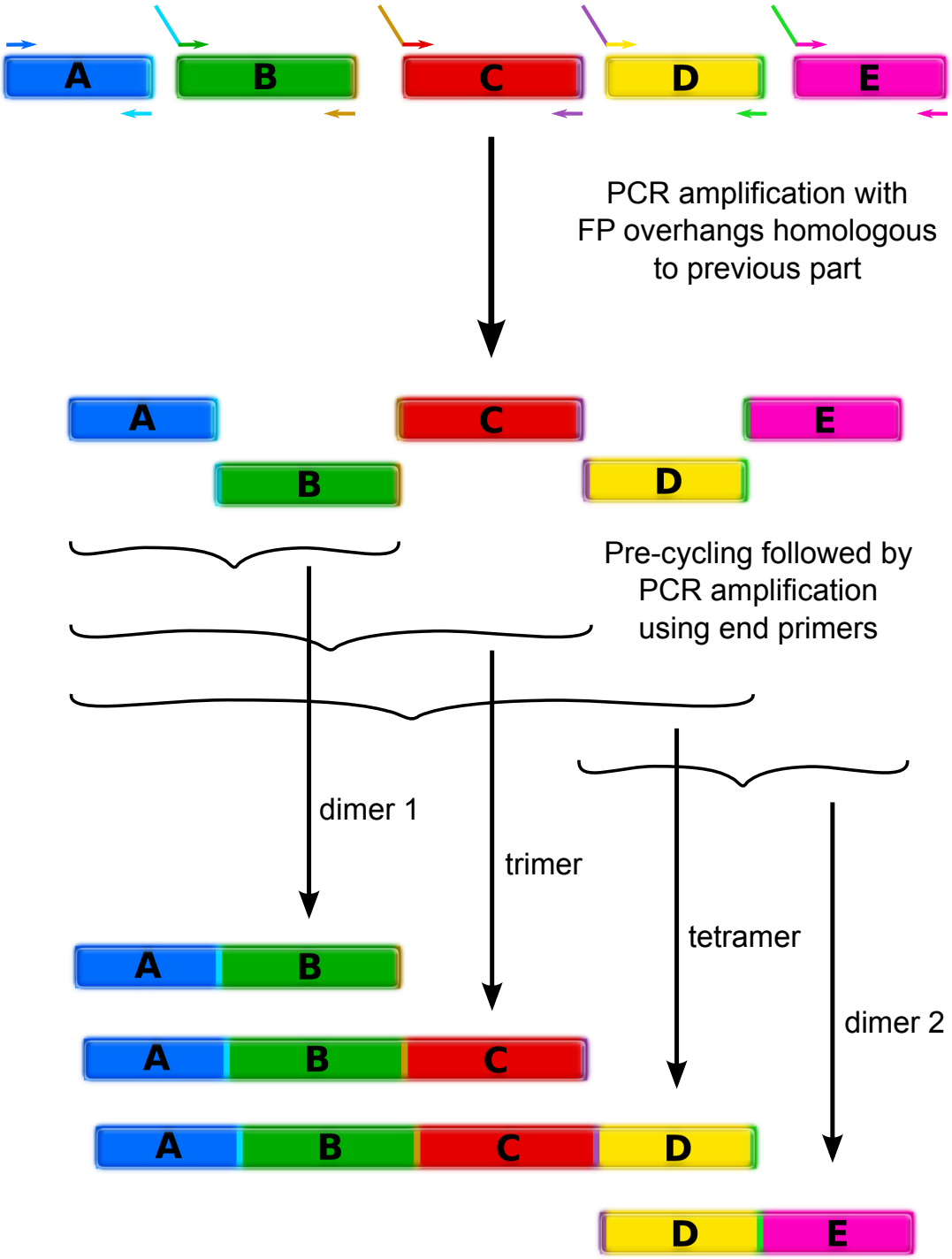

Figure 2.1: A schematic representation of the assembly method used for building our constructs. Monomers are built using FPs with overhangs homologous to the previous piece. These monomers can then be mixed in different combinations to yield various multimers after pre-cycling and amplification with end primers. This strategy generates pieces with large areas of homolgy—a whole gene, for example—that would increase the efficiency of TAR cloning.

cells were placed in a solution containing 33% w/v polyethylene glycol (PEG), 100 mM lithium acetate (LiAc), 300 µg/mL salmon sperm ssDNA, and 200 ng of each multimer in ddH_2O. These were thoroughly mixed by a vortexer and incubated in a water bath at 42°C for 40 min. Cells were washed and those being transformed with an auxotrophic marker were placed on selection plates immediately, whereas those with a drug resistance marker were grown in YPD media for 4 hours before being placed on drug plates.

Regarding the DNA transformed into cells, two approaches were taken. Depending on the number of parts, dimers, trimers, or tetramers were generated such that each would have an area of homology equal to one part (>100 bp) to their adjacent multimers (e.g. tetramer and dimer 2 of Figure 2.1). For areas of homology larger than 40 bp, *S. cerevisiae* can combine multiple fragments [147] through its DNA repair pathway. We always designed the first and the last parts to contain >200 bp homology to our target site for efficient genomic integration.

2.2.2 Isolation of Genomic DNA

A phenol-chloroform method for extraction of yeast genomic DNA was applied. In short, overnight cultures of cells were centrifuged and washed twice (as above). Cells were resuspended in a 1:1 mixture of breaking buffer (2% v/v Triton X-100, 1% w/v SDS, 100 mM sodium chloride, 10 mM Tris-HCl, 1 mM EDTA) and a phenol:chloroform:isoamyl alcohol (25:24:1) solution. 300 mg of acid-washed glass beads were added to the mixture, and the tube was placed in a bead beater for 3 min. TE buffer was added to the resulting suspension, and it was spun down in a microcentrifuge device (Centrifuge 5415 D, Eppendorf) for 5 min at 13000 × g to remove cell debris and beads. The DNA within the supernatant was precipitated with excess 100% ethanol. DNA was collected by microcentrifugation, as described, and treated with RNase A, for 10 min at 37°C, after resuspension in TE buffer. Genomic DNA was once again precipitated as previously outlined and resuspended in TE

buffer.

The genomic DNA yielded from this procedure was used for PCR amplification of desired sequences. The coding sequences (CDS) of both TFs, as well as areas of homology to upstream and downstream of genes of interest, were amplified from genomic DNA thus isolated. Furthermore, after initial screening of successful transformants, a number of them would undergo isolation of genomic DNA for PCR-based confirmation of correct integration.

2.3 Strains and Growth Conditions

2.3.1 Strains

In total, eight strains were generated during this study (see Table 3.1 for full genotypes) from the parental BY4741 strain (EUROpean Saccharomyces Cerevisiae ARchives for Functional analysis, EUROSCARF).

- **WT:** This strain was created by integrating a *yEGFP* CDS directly downstream of the *PDR5* gene. An 8 aa linker (GDGAGLIN) was placed between Pdr5 and yEGFP to maximize the latter's fluorescence [148]. A KanMX cassette was placed downstream of *yEGFP* for drug selection on plates containing 200 μg/mL G418. All other strains were built in this background.

- ***pdr1*Δ and *pdr3*Δ:** A *URA3* expression cassette was obtained from the pRS406 plasmid. Homology sequences (at least 270 bp) upstream and downstream of either *PDR1* or *PDR3* were amplified and attached to the *URA3* cassette to form dimers (two for each strain). The two appropriate dimers for the deletion of each gene were co-transformed in WT cells. Positive transformants were selected by growth on synthetic complete (SC) media without uracil.

- ***pdr1*Δ*pdr3*Δ:** A *HIS3* expression cassette was amplified from the pRS403 plasmid and was trimerized to the upstream and downstream homology sequences of *PDR1*. This trimer was transformed into *pdr3*Δ cells, which were then grown on SC media without histidine to select for successfully transformed colonies.

- **2×*PDR1* and 2×*PDR3*:** The CDS of either *PDR1* or *PDR3* was amplified from isolated genomic DNA of BY4741. For each transformation, a tetramer and a dimer were produced. The tetramer consisted of an area of homology immediately upstream of the gene to be replaced (*PDR3* or *PDR1*), the CDS of the gene to be integrated (*PDR1* or *PDR3*, respectively), the reverse terminator of *S. cerevisiae ACT1* gene, and the *HIS3* expression cassette. The dimer was made up of the *HIS3* expression cassette and a homology area immediately downstream of the gene to be replaced. For each strain, the appropriate tetramer and dimer were co-transformed in the corresponding background strain (*pdr3*Δ or *pdr1*Δ, respectively). Transformants which could grow on SC media without histidine, were replica plated onto SC media lacking uracil to identify and discount false positives.

- ***pdr1*Δ/p3-*PDR1* and *pdr3*Δ/p1-*PDR3*:** The dimers used to create *pdr1*Δ or *pdr3*Δ were co-transformed into 2×*PDR1* or 2×*PDR3*, to knock out the native *PDR1* or *PDR3* gene, respectively. Selection of successful transformants was carried out on SC media lacking uracil.

After each transformation, five colonies were selected and their genomic DNA was isolated. The isolated DNA was used for PCR confirmation of correct integration. Primers were designed outside the areas of homology for each target, as well as within the integrant and the target. Correct integration was confirmed if a PCR product with a correct size was obtained using integrant primers, and no PCR product was present when using target primers. One colony, from those with PCR-confirmed integration, was arbitrarily chosen and frozen at −80°C in YPD supplemented with 15% glycerol.

2.3.2 Growth Conditions

- **Liquid media:** All liquid media consisted of 2% w/v yeast extract and 4% w/v bacteriological peptone (YP) in ddH_2O. YP glycerol/ethanol (YPGE): 3% v/v glycerol and 3% v/v ethanol were added to YP; YP galactose (YPgal): 2% w/v galactose was added to YP; YP dextrose (YPD): 2% w/v glucose was added to YP; 2×YPD: double the amounts of yeast extract and bacteriological peptone were used.

- **Chemicals:** Cycloheximide (#C-6255, Sigma Chemical Company) was dissolved in YPgal to form a stock of 1 mg/mL and was diluted to reach indicated final concentrations. Nocodazole (#13857, Cayman Chemical) was dissolved in dimethyl sulfoxide, DMSO, to form a stock of 5 mg/mL. All dilutions of the drug were maintained in a final concentration of 1% DMSO v/v. Propidium iodide, PI (#P4170, Sigma), was prepared at a stock concentration of 1 mg/mL in a 50 mM sodium citrate buffer and was added to each sample to a final concentration of 5 μg/mL.

2.4 Flow Cytometry and Cell Sorting

A CyAn ADP 9 Analyzer (#CY20130, Beckman Coulter, Inc.) was employed for all flow cytometry experiments. Both fluorophores were excited by a 488-nm solid state laser; yEGFP fluorescence was detected with a 530/40 filter, while PI fluorescence was detected by a 613/20 filter. A MoFlo Astrios Flow Cytometer Cell Sorter (A66831, Beckman Coulter, Inc.) was used for all sorting experiments. A 488-nm solid state laser excited fluorescence of yEGFP, which was detected with a 513/26 filter.

- **Flow cytometry:** Cultures were grown overnight and then diluted to an OD_{600} of 0.05 in appropriate media. They were placed in 96-well plates and grown at 30°C in a shaking incubator. All cells were initially grown for at least 3 hr; for samples treated with a drug, it was added to its working concentration after this growth period.

Samples were diluted 10X in 50 mM sodium citrate buffer, containing PI where indicated, and placed in clean 96-well plates. Samples were mechanically collected and delivered to the cytometer by a HyperCyt Autosampler (IntelliCyt Corp.). For experiments taking place over several days, samples were diluted in their respective media to an OD_{600} of 0.05 once every 12 hours. All Flow Cytometry Standard file formats (.fcs) were analyzed with the FlowJo software (Tree Star Inc.), which was also used for the creation of all histograms.

- **Cell sorting:** For sorting before drug treatment, an overnight culture of cells was diluted to an OD_{600} of 0.15 and grown for 3 hr. For sorting after drug treatment, cells treated with drug were centrifuged and washed twice with YPgal media. They were then allowed to grow for 6 hr in YPgal media in a shaking incubator at 30°C. Samples were sorted based on yEGFP levels, and the gating strategy is described in the Results section (Figure 3.3). The final number of cells collected from each gate was recorded for each sample.

2.5 Spot Assay

Samples were prepared in one of two ways depending on their source. Those from sorting experiments contained sheath fluid and were spun down in the microcentrifuge for 30 s at 13000 $\times$ g. They were diluted in YPgal media to a density of 1×10^6/mL. Those from overnight cultures were diluted to the same density based on their OD_{600}. These samples were incubated at 30°C for one hour. Afterwards, three sequential 10X dilutions were prepared in YPgal for each sample. A 3.6 µL spot of each dilution, as well as the main sample, was placed on plates with or without drug. Plates were incubated at 30°C for 2 to 6 days depending on the condition and were photographed when at least one sample had reached full growth.

Chapter 3

Results

3.1 Characterization of *PDR5* Expression

3.1.1 Reporter Construction and Optimization of Conditions

In order to quantify the level of *PDR5* expression in each cell, we decided to use a strain of yeast that contains a fluorescence tag directly fused to Pdr5. A library of budding yeast GFP-tagged proteins is available; however, the GFP protein used in these strains is not codon optimized for *S. cerevisiae* [149]. Therefore, we decided to label Pdr5 with a copy of yEGFP, *de novo*, in a BY4741 strain (see Table 3.1). *yEGFP* was fused to the coding sequence (CDS) of *PDR5* using homology-based transformation-assisted recombination (TAR) cloning. An area of homology to the C-terminal of *PDR5*, several hundred bp long, was amplified using primers that would exclude the stop codon. Another area of homology upstream of the stop codon was also amplified to ensure efficient integration of the construct in that position. These two areas of homology, as well as the *yEGFP* CDS and a selection marker (KanMX), were fused to each other in a pairwise fashion, using overlap extension PCR, and then transformed into the *S. cerevisiae* BY4741 strain, as described in Methods (Figure 3.1). Correct integration into the target site was confirmed

Figure 3.1: The *PDR5-yEGFP* construct used to report on the level of Pdr5. The construct was integrated into the genome of yeast BY4741 strain, downstream of *PDR5* using the two-step overlap extension PCR and TAR cloning. P5up: the area of homology to the C-terminal of *PDR5* gene up to, but excluding, the stop codon; P5dw: the area of homology downstream of *PDR5* stop codon.

using PCR amplification from isolated genomic DNA of transformants which were able to grow on G418-containing plates.

3.1.2 Flow Cytometry Analysis of *PDR5-yEGFP* Expression under Various Conditions

The expression level of *PDR5* is closely linked to growth and has been shown to depend on the carbon source [116]. Therefore, we investigated the expression profile of Pdr5-yEGFP in presence of three different carbon sources to establish the optimal conditions for our experiments. Glycerol and ethanol are two sources commonly used together in order to create non-fermenting conditions for *S. cerevisiae*. Glucose and galactose are both fermentable, but the BY4741 strain of *S. cerevisiae* does not use galactose anaerobically due to a *gal2-* deletion, creating a unique growth condition.

Accordingly, flow cytometry analysis showed that the level of Pdr5-yEGFP in this strain did not increase much in cells growing with glycerol/ethanol, while a marked increase was detected when cells were grown in glucose (Figure 3.2A). Furthermore, increasing concentrations of both glucose and galactose (up to the commonly used 2% w/v) led to higher levels of Pdr5-yEGFP in both conditions, but the highest level of Pdr5-yEGFP in galactose was lower than that of glucose (Figure 3.2B). Because of the lower basal induction of *PDR5-yEGFP* by galactose compared to glucose, as well as the higher growth rate with

Table 3.1: List of yeast strains.

Strain	Genotype
BY4741	S288C[a]: *MAT***a**; *his3*Δ*1*; *leu2*Δ*0*; *met15*Δ*0*; *ura3*Δ*0*
WT	BY4741: *PDR5-yEGFP-KanMX*
*pdr1*Δ	WT: *pdr1*Δ::*URA3*
*pdr3*Δ	WT: *pdr3*Δ::*URA3*
*pdr1*Δ*pdr3*Δ	*pdr3*Δ: *pdr1*Δ::HIS3
2×*PDR1*	*pdr3*Δ: *ura3*Δ::*PDR1-rtACT1-HIS3*
2×*PDR3*	*pdr1*Δ: *ura3*Δ::*PDR3-rtACT1-HIS3*
*pdr1*Δ/p3-*PDR1*	2×*PDR1*: *pdr1*Δ::*URA3*
*pdr3*Δ/p1-*PDR3*	2×*PDR3*: *pdr3*Δ::*URA3*

[a] The parental strain from which the indicated strain was derived is shown before the colon.

it compared to glycerol/ethanol, we chose to add galactose as the carbon source to our media (rich media hereafter) for the remaining experiments. Curiously, we noticed that a high-expressing subpopulation (HES) was present in samples that were not treated with drug (Figure 3.2C). This HES constitutes at least 1% of the total population growing in log phase, and its distribution is distinctly discernible from that of a low-expressing subpopulation (LES) comprising the remaining of the population.

Next, we investigated the response of this strain to cycloheximide and nocodazole, two substrates of Pdr5. Cycloheximide is a cytotoxic organic compound, with a relatively simple structure, which inhibits eukaryotic protein synthesis by occupying the E-site of the ribosomal complex and blocking its translocation along the mRNA [150]. Nocodazole interferes with microtubule formation and spindle assembly during mitosis by binding to tubulin dimers and inhibiting their polymerization [151, 152]. Cycloheximide is extensively used as a reporter on Pdr5 activity and has been shown not to be extruded by other major

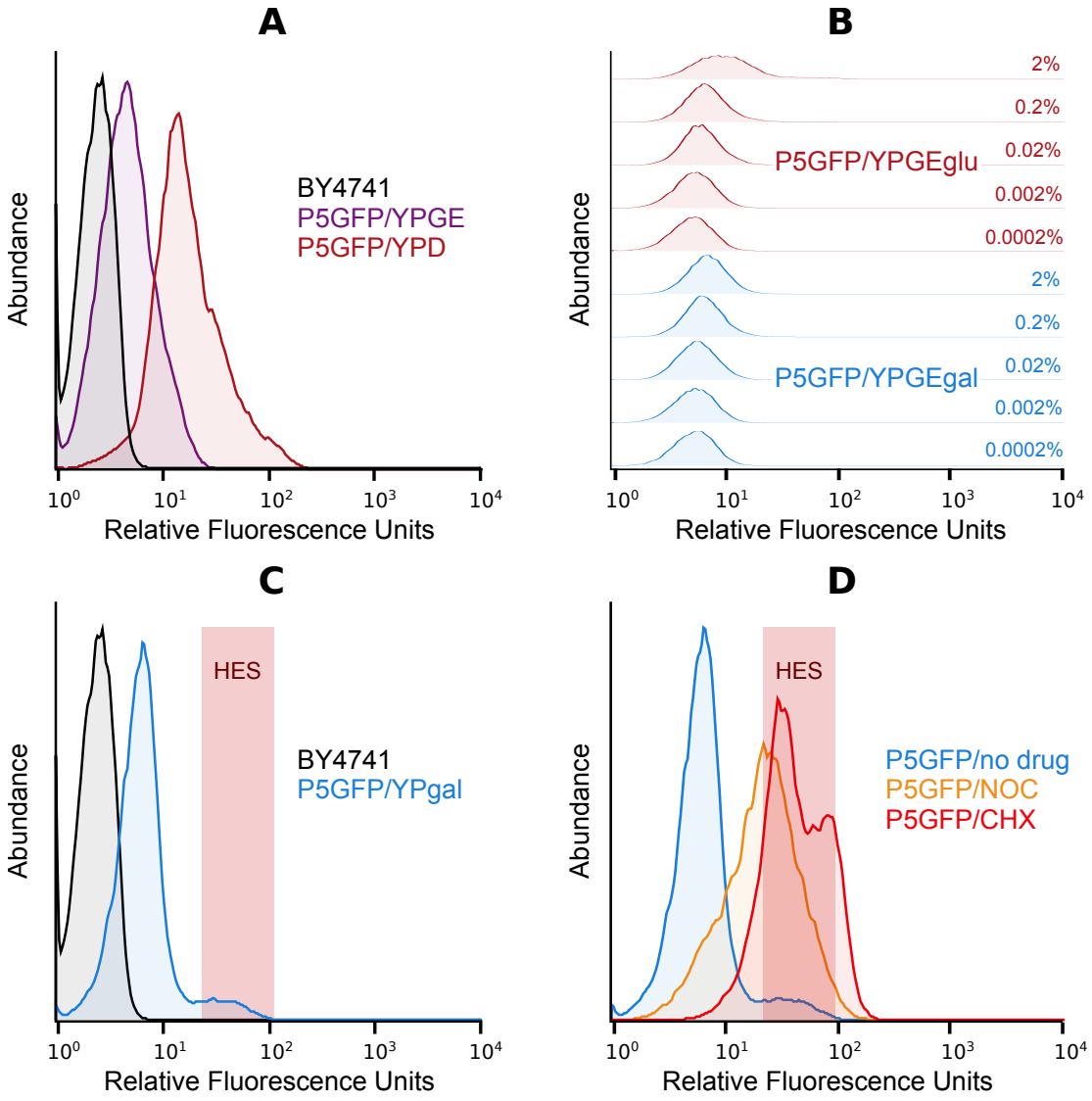

Figure 3.2: Characterization of *PDR5-yEGFP* expression profile under different conditions. A) The Pdr5-yEGFP levels in WT strain when grown in YP with 2% glucose (maroon) or glycerol/ethanol (violet) compared to autofluorescence of parental strain with no yEGFP. B) A rise in the level of Pdr5-yEGFP with higher concentrations of either glucose (maroon) or galactose (blue) up to a final concentration of 2% w/v. Cells were grown in YPGE with increasing amounts of either glucose or galactose, as indicated. C) Basal level of Pdr5-yEGFP when grown in rich media compared to BY4741 autofluorescence. The Pdr5-yEGFP profile comprises of two differentially expressing subpopulations; the high-expressing subpopulation (HES) is highlighted. D) Significantly higher levels of Pdr5-yEGFP after growth in presence of either nocodazole, NOC, (orange) or cycloheximide, CHX, (red) compared to basal levels. The cells were grown in 5 µg/mL of NOC or 0.1 µg/mL of CHX for 52 hours and kept in log phase by diluting in fresh drug-containing media every 12 hours.

ABC transporters in *S. cerevisiae* [118], whereas nocodazole—among other azoles—can be removed by Pdr5, as well as some other factors [153, 154]. As expected, the level of Pdr5-yEGFP increased significantly after long exposure to either drug (Figure 3.2D). After 52 hours of treatment, cycloheximide induced higher levels of Pdr5-yEGFP than nocodazole, both of which were used in sublethal concentrations that would allow reasonable growth. Since cycloheximide is transported outside the cells exclusively by the action of Pdr5, we elected to use this drug for the rest of this study.

3.1.3 Properties of HES and LES

Identification of a distinct subpopulation of *S. cerevisiae* cells that expressed *PDR5-yEGFP* at higher levels than the rest of the population prompted us to consider the role and function of the HES in drug resistance. It is reasonable to expect that those cells with a higher level of Pdr5-yEGFP would be able to more efficiently remove a drug substrate of Pdr5 and survive in its presence. In particular, the average level of Pdr5-yEGFP in the HES coincides well with its average level in the whole population of drug treated cells (Figure 3.2D).

To test this hypothesis, a log-phase population of WT cells harbouring the *PDR5-yEGFP* construct was enriched for the HES and the LES using fluorescence-activated cell sorting (FACS). The HES and the LES were collected with gates set at the two extremities of the Pdr5-yEGFP expression profile, as indicated in Figure 3.3A, which contained approximately 1% and 90% of the total population, respectively. Flow cytometry analysis of the two enriched subpopulations after sorting (Figure 3.3B) revealed that while the separation was not perfect, the high-gated sample was ∼60% enriched for HES and the low-gated sample was ∼80% enriched for LES. We maintained the sample enriched for HES in rich media for 42 hours, at which time the population re-established its original distribution (Figure 3.3C). The percentage of cells in the HES progressively decreased to

asymptotically approach the value of 1% with a half-life of about 11 hours.

Both the high-gated and low-gated samples were analyzed for their ability to survive on cycloheximide-containing plates. Ten-fold dilutions of each sample, starting from the same cell density—based on cell count provided by the cell sorter—were spotted on rich-media plates with or without cycloheximide. Figure 3.4 clearly shows the superior capability of the HES-enriched sample to survive and grow on drug-containing plates when compared to the LES-enriched one. Furthermore, the HES-enriched sample grew better than the unsorted population in the presence of drug. The growth advantage of HES-enriched samples appears to be directly related to their higher average level of Pdr5-yEGFP since they grew slower in the absence of cycloheximide than the LES-enriched and unsorted samples, which grew equally well.

3.1.4 Pdr5-yEGFP Response to Cycloheximide Treatment

Investigation of the *PDR5-yEGFP* expression profile in this strain of *S. cerevisiae*, in the absence of any drug, demonstrated the presence of two subpopulations with distinct phenotypes whose presence or absence has strong implications for the ability of cells to survive drug treatment. Therefore, we wondered if the dynamics of Pdr5-yEGFP induction would be consistent with the case of a bimodal population in which these subpopulations may play a role. Initially, we investigated the increase in mean levels of Pdr5-yEGFP when grown in liquid cultures of rich media supplemented with cycloheximide. Under these conditions, for cells maintained in log phase, the rate of increase in levels of Pdr5-yEGFP was modest at the beginning, but grew over time, to finally reach a plateau after more than 3 days. The resulting sigmoidal time-course is shown in Figure 3.5A. We also followed the dynamics of Pdr5-yEGFP relaxation from its highest level after removing the drug. This experiment was designed mainly to investigate the presence or absence of memory in the *PDR5-yEGFP* expression system. Presumably, if a mechanism for generation of memory

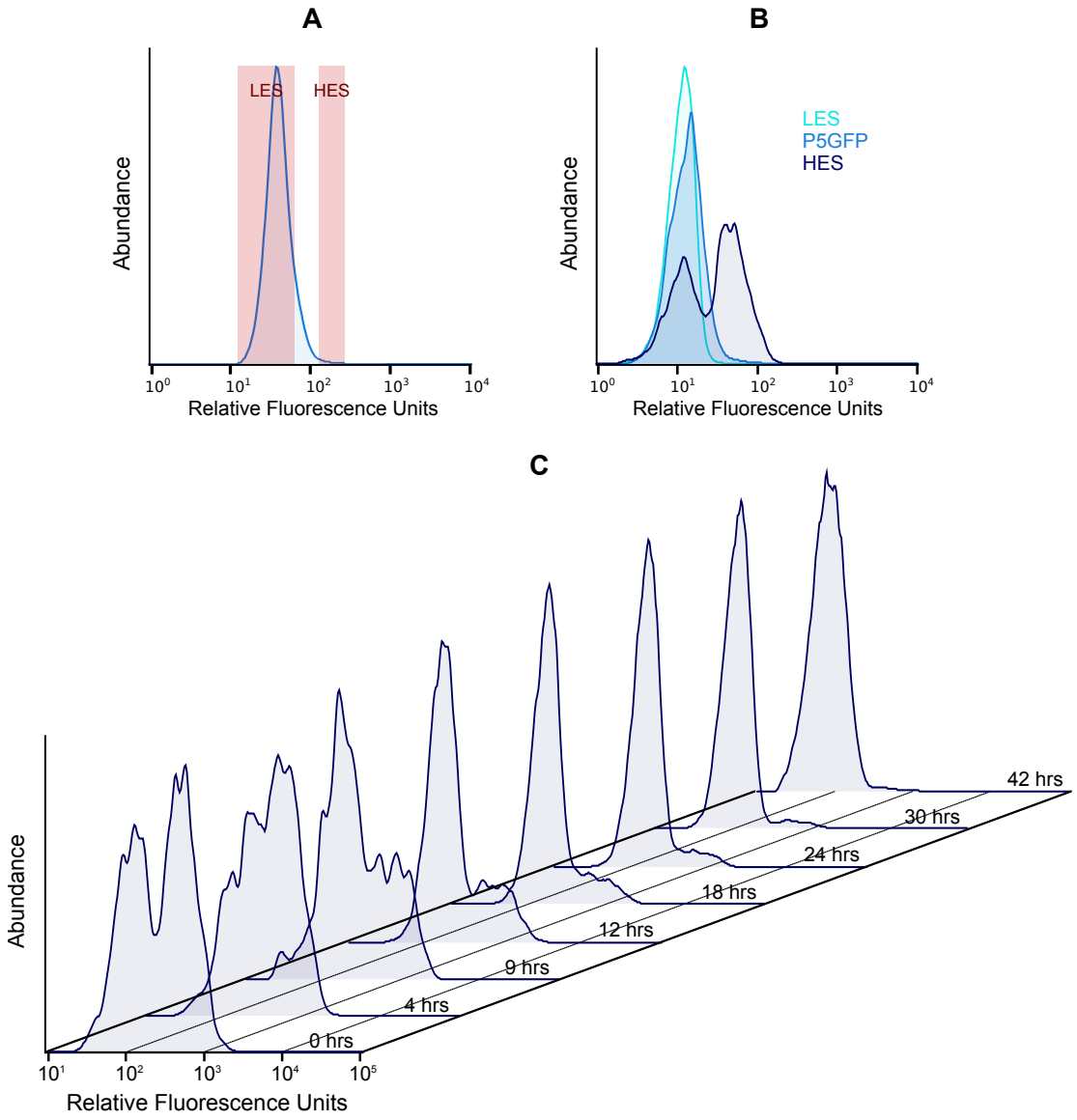

Figure 3.3: Analysis of HES and LES properties through FACS enrichment of these subpopulations. A) Placement of sorting gates for enriching HES and LES containg samples. Approximately 1% and 90% of the total population, respectively, were collected in each gate. B) Flow cytometry analysis, immediately after sorting, demonstrates enrichment for HES in the high-gated sample (dark blue) and for LES in the low-gated sample (cyan) compared to the unsorted population (blue). C) The population profile of the HES-enriched sample shifts gradually to its original form after 42 hours of growth in rich media. Cells were kept in log phase through dilution in fresh media at 12-hour intervals.

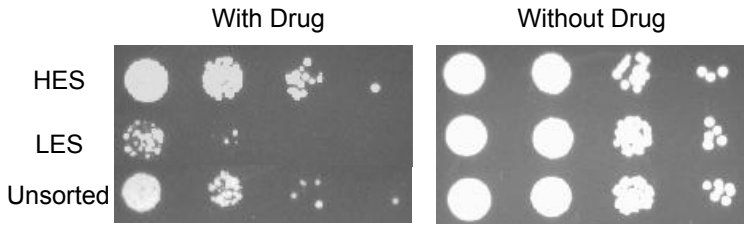

Figure 3.4: Spot assay of HES-enriched, LES-enriched, and unsorted samples in the presence or absence of drug. Sorted and unsorted cells were diluted to the same density, and ten-fold dilutions of these were spotted on rich media plates with or without 0.1 µg/mL cycloheximide.

exists, the high expression level will linger for a time, the length of which is dependent on the strength of said mechanism. Conversely, a linear decrease in the level of Pdr5-yEGFP would be expected if no memory existed. Flow cytometry analysis of Pdr5-yEGFP levels after removal of drug, indeed, demonstrates persistence of higher levels of Pdr5-yEGFP for at least 12 hours after release from cycloheximide. The inset of Figure 3.5C shows this 12-hour delay in reduction of mean Pdr5-yEGFP levels. However, what the change in the mean level of Pdr5-yEGFP fails to capture is the mechanism by which it comes to be. The average Pdr5-yEGFP levels decrease not due to a gradual shift in these levels within the whole population, but as a result of a decrease in the number of cells of an HES and the corresponding increase in those of an LES (Figure 3.5C).

Two processes can plausibly give rise to such dynamics. First, the cells within the LES may enjoy much higher fitness in rich media than those in HES, and thus, outcompete the latter and completely overtake them. Second, elevated expression of *PDR5-yEGFP* may be reversible, allowing cells of the HES to return to basal levels of Pdr5-yEGFP after a lag period in the high expression regime. In order to assess the possibility of these two alternatives, we evaluated the likelihood of survival of a seed LES during drug treatment to reestablish itself after drug removal, as well as the ability of HES cells to grow in rich media. Cells were exposed to cycloheximide for 72 hours followed by drug removal and growth in rich media for a further 6 hours. The resulting population had a bimodal

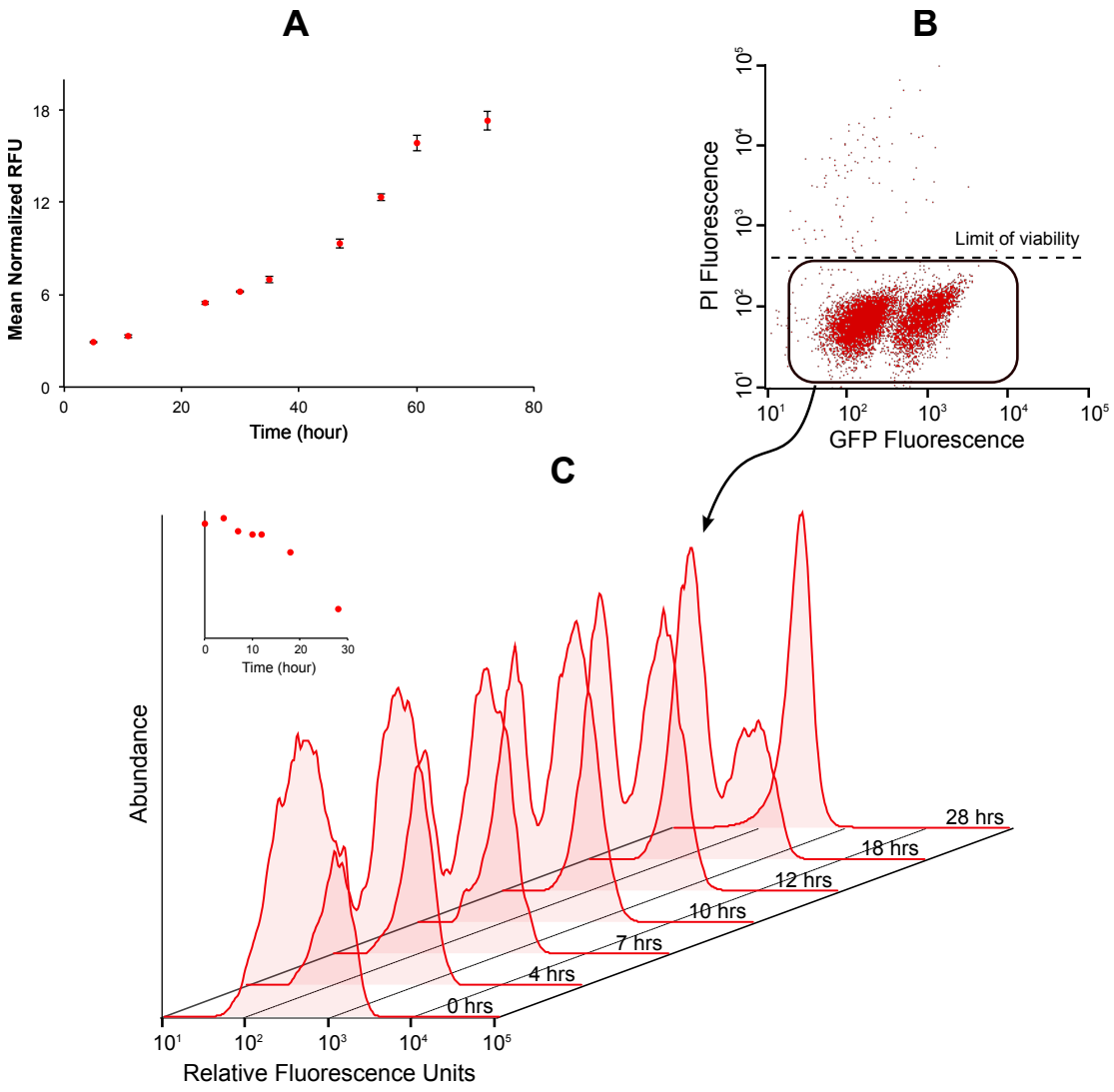

Figure 3.5: Pdr5-yEGFP response to cycloheximide treatment and removal. A) Mean levels of Pdr5-yEGFP increase sigmoidally over time. Cells were incubated with 0.1 µg/mL cycloheximide for 72 hours and their fluorescence was measured at 6- or 12-hour intervals using flow cytometry. Mean values at each time point were normalized to autofluorescence of BY4741 cells under the same drug conditions. Error bars are standard deviation of technical triplicates. B) An example of a two dimensional dot plot where yEGFP fluorescence is given by the abscissae and PI fluorescence is given by the ordinates. Cells above the dashed line accumulate PI and are considered to be inviable. This profile corresponds to the population 18 hours after drug removal. C) The evolution of Pdr5-yEGFP population profile over time after removal of cycloheximide and growth in rich media. Cells were grown in rich media after 72 hours of 0.1 µg/mL cycloheximide treatment and were maintained in log phase by dilution in fresh media at 12-hour intervals. Inset: Normalized mean levels of Pdr5-yEGFP obtained from shown histograms. Values were normalized as in A).

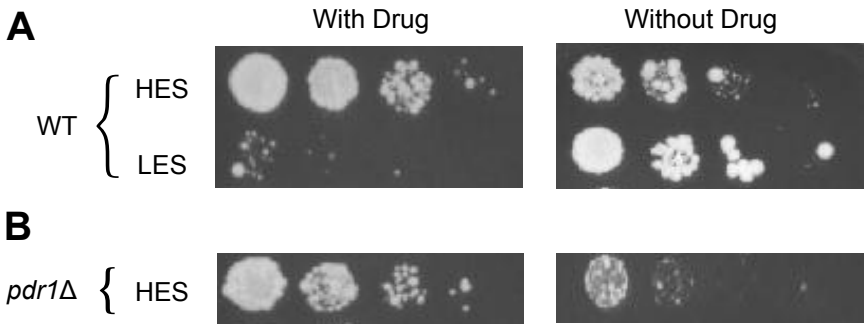

Figure 3.6: Spot assay of HES-enriched and LES-enriched samples after drug removal from (A) WT and (B) *pdr1*Δ cells in the presence or absence of cycloheximide. Cells were grown in rich media for 6 hours after a 72-hour treatment in 0.1 μg/mL cycloheximide. These populations were sorted using high and low yEGFP gates to obtain HES- and LES-enriched samples for WT and HES-enriched samples only for *pdr1*Δ (since no appreciable amount of LES was present for this strain at that time point). Cells were spotted on plates with or without 0.1 μg/mL cycloheximide as in Figure 3.4.

distribution of Pdr5-yEGFP-expressing cells (similar to that of Figure 3.5C). The sorted HES and LES were then spotted on rich-media plates with or without drug (Figure 3.6A). As previously observed, the LES sample was greatly disadvantaged in presence of the drug. In fact, in this case, the LES sample was almost completely unable to grow on drug-containing plates, presumably due to higher enrichment of each subpopulation compared to the previous experiment. Furthermore, the sample enriched in HES had a clearly lower fitness on rich media alone. However, its ability to grow on these plates indicated that it has a reasonable fitness in rich media, albeit lower than the LES sample. We also incubated cells with propidium iodide (PI) to directly measure the viability of each subpopulation. PI is an ionic DNA-intercalating dye that is excluded from the cytoplasm of cells with intact membranes. Thus, it is commonly used to report on membrane integrity, as a proxy for cell viability, in many organisms [155]. Figure 3.5B shows a bimodal population of cells—18 hours after drug removal—expressing Pdr5-yEGFP and stained with PI. Even though more than 35% of the cells are within HES, none of those are detected beyond the threshold above which cells are considered to be inviable.

3.2 Contribution of *PDR5* Regulatory Network to Its Expression Dynamics

PDR5 expression is activated by two paralogous TFs, Pdr1 and Pdr3, which are arranged such that they give rise to a C1FFL motif with a positive FBL nested within it (Figure 1.5B). As outlined previously, both these motifs enhance stochastic variability in their target genes and result in a delayed OFF response. Consequently, we set out to investigate the role of these two TFs and the network components in the response of Pdr5-yEGFP to cycloheximide.

3.2.1 Deletion of *PDR1* and *PDR3*

We began with generating three mutants, bearing deletions of *pdr1*, *pdr3*, or both (Figure 3.7A). To create single-deletion strains, *pdr1*Δ and *pdr3*Δ, either gene was displaced by insertion of a *URA3* expression cassette with large sequences homologous to regions upstream of the gene's start codon and downstream of its stop codon. Transformation of the cassette and these homologous regions (in two pieces) was performed as described in the Methods section. The deletion of each gene was established by PCR-based confirmation of positive transformants using appropriate primers. The double mutant, *pdr1*Δ*pdr3*Δ, was similarly constructed by knocking out *PDR1* in the *pdr3*Δ strain with a *HIS3* expression cassette.

Based on the current consensus about the regulation of *PDR5* by these two TFs, the *pdr3*Δ strain would include only a simple, direct-activation network controlling the *PDR5-yEGFP* expression. We expected that this strain would demonstrate lower heterogeneity in expression, as a result of losing both C1FFL and FBL motifs. However, its response to drug should not greatly differ from that of the WT given that Pdr1 is considered to be the master regulator of *PDR5* with evidence of its binding and induction by cycloheximide.

On the other hand, the *pdr1*Δ strain, would comprise only of the positive FBL driven by Pdr3. Accordingly, we anticipated that while the expression level of *PDR5-yEGFP* should be quite low, its variability would be much higher than at least *pdr3*Δ.

The flow cytometry data obtained from these three strains confirmed some of our predictions while disproving others. The *pdr3*Δ strain mostly met these expectations; in the absence of any drug, its levels closely resembled that of WT, and its HES decreased by almost 10-fold compared to that of WT (Figure 3.7B). In contrast, the *pdr1*Δ strain had a surprisingly high expression level. Since the *pdr1*Δ*pdr3*Δ mutant showed only slightly higher levels of Pdr5-yEGFP than cellular autofluorescence, it must be concluded that even if another mechanism of *PDR5* activation is present, it is not nearly as strong. Therefore, it appears that Pdr3 is either able to activate *PDR5* to a level similar to that of WT when present at a much lower concentration than Pdr1 (∼10 fold [137]) or that *PDR3* itself is activated by some other factor in the absence of Pdr1. More interestingly, when we focused on the HES of *pdr1*Δ cells, not only was it larger than those of both *pdr3*Δ and WT strains (more than 20 and 2 folds, respectively), its mean level of Pdr5-yEGFP was approximately 30% larger than that of the WT (FIgure 3.7C). This clue is consistent with the first scenario proposed above, in which Pdr3 is stronger than Pdr1 and can activate the expression of *PDR5* more strongly than the latter.

Moreover, we repeated the spot assay experiment with the *pdr1*Δ strain (the only mutant strain with an appreciable HES). Similar to the WT case, the HES-enriched sample of *pdr1*Δ cells was able to survive not only better than the LES-enriched sample, but also the unsorted one (Figure 3.8). Yet, the HES-enriched sample was at a more distinguishable disadvantage compared to the other two samples in a way reminiscent of the WT HES after drug treatment. This outcome is potentially due to the higher level of Pdr5-yEGFP in the HES of *pdr1*Δ cells. Consistent with these results, the HES-enriched sample of *pdr1*Δ that was sorted after 72 hours of drug treatment grew well on cycloheximide-containing plates. On the other hand, this one had a lower fitness—even lower than the WT HES-enriched

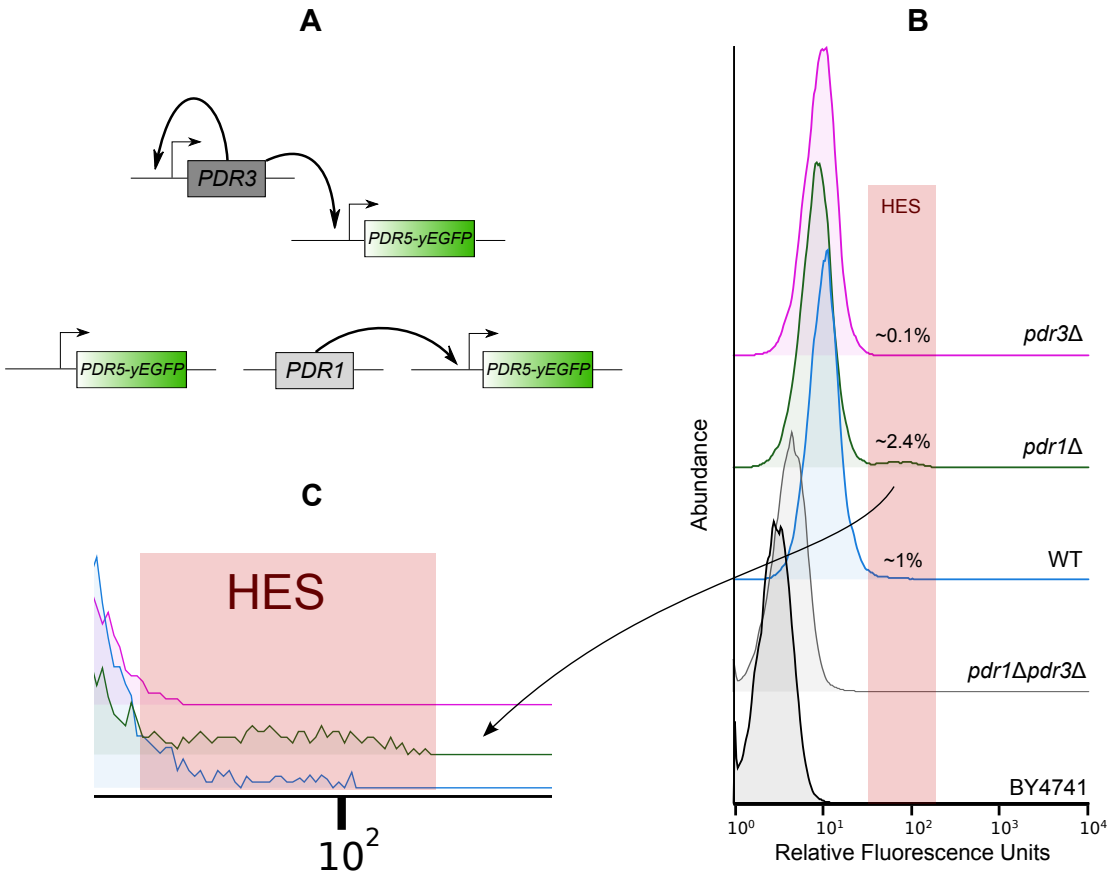

Figure 3.7: The *PDR5-yEGFP* expression profile in *pdr3*Δ, *pdr1*Δ, and *pdr1*Δ*pdr3*Δ strains compared to that of WT during log-phase growth in rich media. A) A schematic representation of the network architecture regulating *PDR5* expression in each deletion mutant. B) The population profile of *pdr3*Δ (magenta), *pdr1*Δ (green), *pdr1*Δ*pdr3*Δ (grey), and WT (blue) strains compared to BY4741 autofluorescence (black). These profiles were obtained from cells growing in rich media at log phase using flow cytometry. Proportion of cells in the HES are indicated for each strain (0% when not indicated). The position of this subpopulation is highlighted. C) A magnification of the HES profie for *pdr1*Δ, *pdr3*Δ, and WT strains.

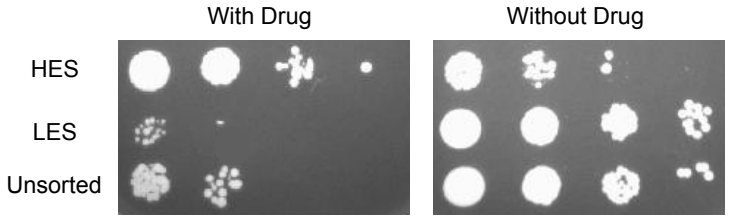

Figure 3.8: Spot assay of HES-enriched, LES-enriched, and unsorted samples of the *pdr1*Δ strain in the presence or absence of cycloheximide. A population of *pdr1*Δ cells was grown in rich media and sorted using high and low yEGFP gates while in log phase. Sorting and spotting were carried out as described in Figure 3.4.

sample—on rich media (Figure 3.6B).

3.2.2 Drug Response of Mutants

The conspicuous phenotype of the *pdr1*Δ strain in the absence of the drug led us to contemplate the possibility that this strain may demonstrate odd behaviour upon treatment with cycloheximide, as well. Initially, we investigated the change in the expression level of Pdr5-yEGFP in all three mutants and compared it to that of WT. As evident in panel A of Figure 3.9, Pdr5-yEGFP levels in the *pdr1*Δ strain become strikingly higher than those of both WT and *pdr3*Δ. While we had predicted, due to its basal expression level and a relatively large HES, that the *pdr1*Δ strain would be able to survive in the presence of cycloheximide, we certainly did not expect its level of Pdr5-yEGFP to be so much higher than WT. Less surprising was the inability of Pdr1 alone (in *pdr3*Δ cells) to reach similar levels of Pdr5-yEGFP as WT since without the feedback on Pdr3, it could not dramatically increase the levels of Pdr5-yEGFP. Also, the sharp switch-like increase in Pdr5-yEGFP levels of the *pdr1*Δ strain is consistent with the positive FBL structure. Another noteworthy observation was the lower initial levels of Pdr5-yEGFP in the first ∼10 hours of drug treatment in the *pdr1*Δ population (to the left of the red dashed line). This is in contrast to the steady increase of Pdr5-yEGFP levels in both WT and *pdr3*Δ cells. After this time, *pdr3*Δ cells do not further increase their levels of Pdr5-yEGFP, unlike

WT cells which do. Therefore, the WT strain appears to possess the hybrid temporal properties of the *pdr1*Δ and *pdr3*Δ strains. These dynamic and temporal differences in *PDR5-yEGFP* expression between *pdr3*Δ and *pdr1*Δ appear to be dependent on Pdr1 and Pdr3, respectively, since the *pdr1*Δ*pdr3*Δ strain did not show any such dynamics.

In addition to measuring the level of Pdr5-yEGFP in cells of each strain, we quantified the proportion of cells in each population that were able to extrude PI at each time point. As mentioned previously, PI is a binary reporter for determining viability of cells. While accumulation of PI only means that a cell's plasma membrane is damaged, this property is often equated to a loss of viability. Furthermore, we have directly observed, using a microfluidics chamber coupled with a time-lapse fluorescence microscopy, that individuals which uptake PI do not resume growth even several hours after removing the drug and adding rich media. Therefore, we considered PI staining to be a good measure for cell survival and defined percent viability to be the proportion of cells that do not fluoresce in presence of PI (see Figure 3.5B for an example). We further established the validity of this measure by killing BY4741 cells using heat—cells did not grow in rich media after treatment—and confirming the ability of PI to differentially stain dead *S. cerevisiae* cells.

The viability of all strains were consistent with a Pdr5-yEGFP-dependent cycloheximide resistance. Accordant with the delay in rising levels of Pdr5-yEGFP in *pdr1*Δ cells, a larger portion of this population loses its viability, within the initial ∼20 hours of cycloheximide treatment, than either the *pdr3*Δ or WT populations. However, as the level of Pdr5-yEGFP in *pdr1*Δ cells elevates dramatically, the proportion of viable cells also increases beyond those of the other strains. Also, percent viability of the *pdr3*Δ strain closely resembles that of the WT population at the beginning of drug treatment. This further highlights the difference in the *PDR5-yEGFP* expression dynamics among the different strains and its contribution to each individual's chances of survival over time. The inability of the *pdr1*Δ*pdr3*Δ strain to increase the expression level of Pdr5-yEGFP in presence of cycloheximide and its almost complete loss of viability at the end of treat-

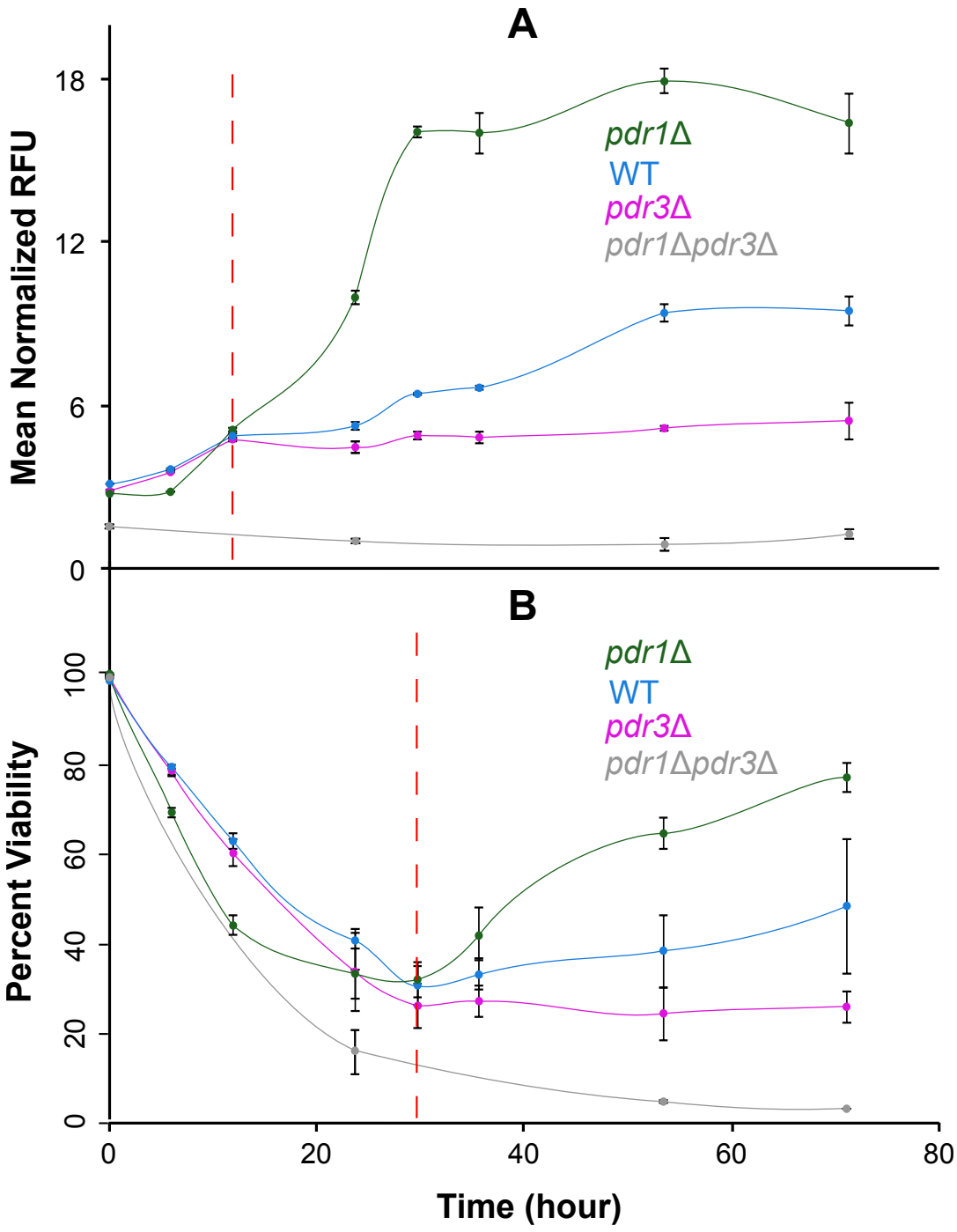

Figure 3.9: The response of *pdr3*Δ, *pdr1*Δ, and *pdr1*Δ*pdr3*Δ strains to cycloheximide treatment compared to WT. The change in (A) the mean levels of Pdr5-yEGFP and (B) percent viability of cells over time in each of *pdr3*Δ (magenta), *pdr1*Δ (green), *pdr1*Δ*pdr3*Δ (grey), and WT (blue) in response to 0.1 µg/mL cycloheximide. *pdr1*Δ*pdr3*Δ cells were sampled at fewer time points since they demonstrated no apparent change. The mean fluorescence obtained from flow cytometry experiments was normalized as described previously. Error bars are standard deviation of technical triplicates. Red dashed lines indicate the time point at which the behaviour of the *pdr1*Δ strain, for the corresponding property of the population, dramatically changes.

ment confirms the need for the Pdr1/Pdr3-dependent expression of Pdr5 to extrude this drug. Indeed, this dependence is not true in the case of nocodazole treatment, where, even though Pdr5-yEGFP remained at its basal levels during the entirety of the treatment in *pdr1*Δ*pdr3*Δ cells, this strain was able to regain its viability, albeit slower than the others (data not shown).

It is interesting to note that, in line with the switch-like dynamics of *PDR5-yEGFP* expression in *pdr1*Δ cells, its expression profile shows a more distinct bimodality in this strain than in WT both during drug treatment and after its removal (Figure 3.10). The HES of the *pdr1*Δ population distinctly increases in proportion over nearly 30 hours (Figure 3.10A). The WT population, however, shows a more gradual increase in Pdr5-yEGFP level where the separation of HES and LES is not as clear as that of the *pdr1*Δ strain. Furthermore, the initial level of HES in the *pdr1*Δ population is larger than that of the WT population (as discussed previously), and the former maintains a higher mean level of Pdr5-yEGFP in its HES throughout the cycloheximide treatment. After an almost complete population switch from LES to HES at 30 hours, the *pdr1*Δ mean level of Pdr5-yEGFP plainly overtakes that of WT.

A similar distinct bimodality of Pdr5-yEGFP levels exists in the *pdr1*Δ strain upon removal of cycloheximide and growth in rich media (Figure 3.10B). It is interesting to see that the total level of Pdr5-yEGFP increases, transiently, after removal of drug (compare the distributions at 0 and 9 hours). While this trend happens in the WT strain, as well (Figure 3.5C), it is more easily detected in the case of the *pdr1*Δ strain. In fact, this effect in the *pdr1*Δ population allows us to easily distinguish between LES and HES noting that almost all of the cells are located within the latter. We believe that this effect is specific to cycloheximide and may be due to a backlog of mRNA caused by this drug's mode of action in blocking translation. The fact that we have not observed such dynamics after release of cells from nocodazole lends some support to this notion. Lastly, one must not overlook the timescale of the change in the population profile of *pdr1*Δ cells. It takes approximately

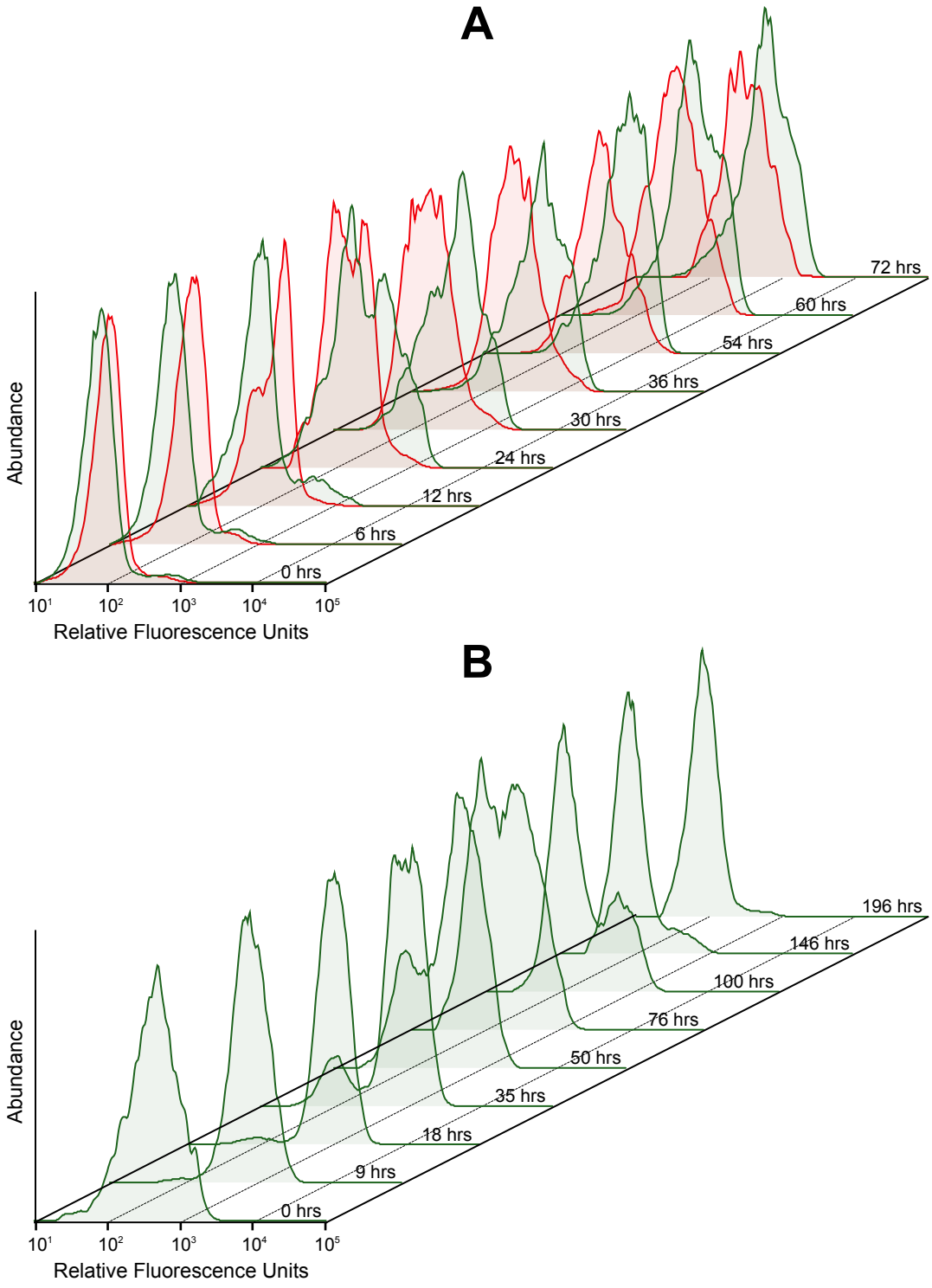

Figure 3.10: Bimodality in the population profile of *pdr1*Δ cells during and after cycloheximide treatment. A) The change in the population profile of Pdr5-yEGFP levels for the *pdr1*Δ (green) and WT (red) strains in 0.1 μg/mL cycloheximide over 72 hours. Histograms of flow cytometry results for yEGFP fluorescence of the two strains are overlaid for each time point. B) The gradual shift in the population profile of *pdr1*Δ cells after drug removal over 196 hours. Cells were grown in rich media after the 72-hour cycloheximide treatment and were maintained in log phase by dilution in fresh media at 12-hour intervals.

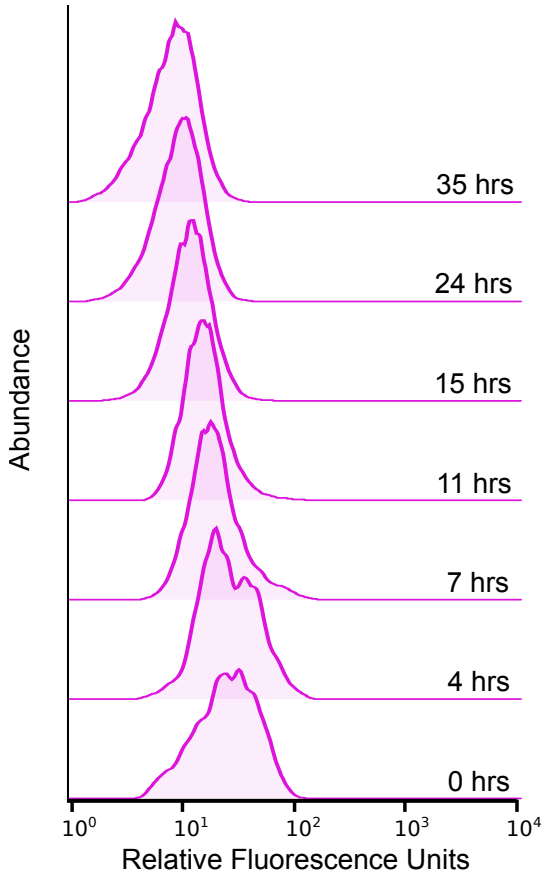

Figure 3.11: Unimodal evolution of the *pdr3*Δ population profile after drug removal. Cells were grown in rich media, and were maintained in log phase, for 35 hours, following a 72-hour treatment with 0.1 µg/mL cycloheximide.

76 hours for *pdr1*Δ cells to reach a 50-50 LES-HES population profile—compared to ∼12 hours for WT cells—and more than a week to reestablish the original population profile before drug treatment—compared to ∼28 hours for WT.

The bimodal decrease in the levels of Pdr5-yEGFP in WT and *pdr1*Δ cells is in stark contrast to the linear dynamics of *pdr3*Δ strain after drug removal. The level of Pdr5-yEGFP in *pdr3*Δ cells lingers for a short time—∼4 hours—after drug removal (Figure 3.11), but this could be due to the mRNA backlog effect invoked to explain the similar phenomenon in the other two strains. After this time point, *PDR5-yEGFP* expression decreases gradually and unimodally until it reaches its basal levels, which it does at ∼15 hours—almost half the time it takes for WT to do so.

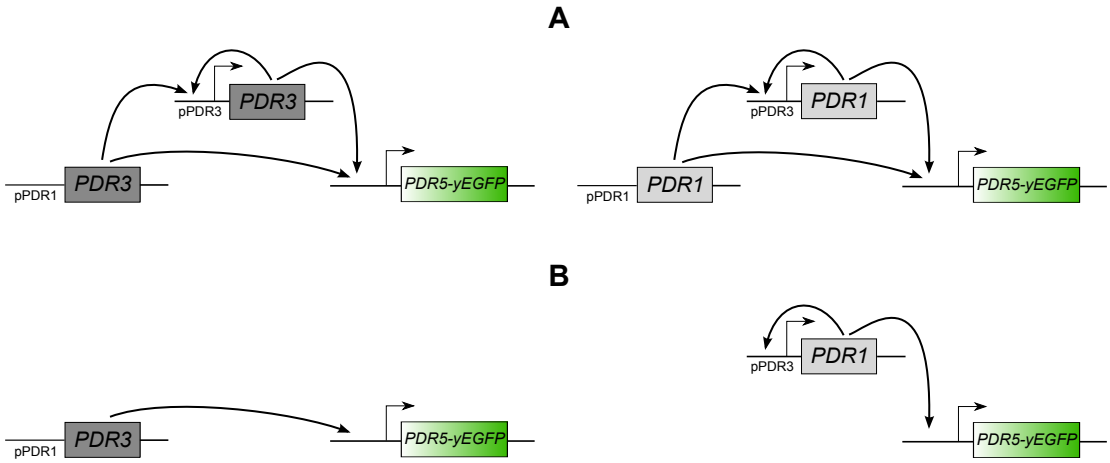

Figure 3.12: Schematic depiction of network variants which contain only one of the two TFs. A) C1FFL with positive FBL achieved by two *PDR3* genes, 2×*PDR3* (left), or two *PDR1* genes, 2×*PDR1* (right). B) Single TF networks driven from the other's promoter. *PDR3* CDS is controlled by the pPDR1 promoter, *pdr3*Δ/p1-*PDR3* (left), or *PDR1* CDS is driven from the pPDR3 promoter, *pdr1*Δ/p3-*PDR1* (right). The native TF is deleted in both cases.

3.2.3 Other Network Variants

The oddly higher levels of Pdr5-yEGFP in the *pdr1*Δ strain compared to WT, and its ability to better survive in prolonged cycloheximide exposure, suggested that Pdr3 may be a stronger activator than Pdr1. Pdr1 and Pdr3 presumably form homo and heterodimers when both are present [134]. Therefore, if Pdr1 had lower activity—either due to lower affinity to DNA or diminished capacity to recruit transcriptional machinery—it would stand to reason that its presence in WT cells would lead to the formation of heterodimers that are less active than Pdr3-Pdr3 homodimers. In an attempt to remove the complication caused by the differential activity of Pdr1 and Pdr3 from the study of their network dynamics, we produced two variants each featuring either Pdr1 or Pdr3 as the only TF in the C1FFL network controlling the activity of Pdr5-yEGFP, illustrated in Figure 3.12A.

The first mutant, 2×*PDR3*, contained two copies of *PDR3*—one driven from its own promoter and the other from the native pPDR1 promoter. This strain was constructed by knocking out the *URA3* expression cassette in the *pdr1*Δ strain with a construct consisting

of the *PDR3* gene attached to a *HIS3* expression cassette. Transformants were grown on synthetic media lacking histidine and correct integration was confirmed using PCR amplification. Furthermore, the integration locus was sequenced by Sanger sequencing to check for potential mutations or substitutions in the newly inserted *PDR3* CDS. Sequencing yielded 69% coverage of the locus, in which no mutations were detected.

The change in the profile of *PDR5-yEGFP* expression during drug treatment in the 2×*PDR3* strain demonstrates an interesting combination of WT and *pdr1*Δ profiles (Figure 3.13). At the early stages of drug treatment this strain behaves similar to WT cells, where its Pdr5-yEGFP levels increase slowly for ∼47 hours until a larger jump in the mean Pdr5-yEGFP levels. This change in the level of Pdr5-yEGFP is unlike the distinctly bimodal behaviour of *pdr1*Δ cells, which gain a sharp increase in their Pdr5-yEGFP levels after constant initial levels. However, by the time the steady-state levels of Pdr5-yEGFP are reached at ∼72 hours, they are very close in both the 2×*PDR3* and *pdr1*Δ strains.

The second mutant, 2×*PDR1*, was constructed in a similar fashion to the former. *PDR1* followed by a *HIS3* expression cassette formed a construct that was integrated into the genome to displace the *URA3* expression cassette of the *pdr3*Δ strain. Sequencing of this locus resulted in 89% coverage, in which no mutations were detected, either.

The mean levels of Pdr5-yEGFP in both the 2×*PDR1* and *pdr3*Δ strains are very close to each other during the 72-hour cycloheximide treatment (Figure 3.13). The change in the population profile of Pdr5-yEGFP in these two strains is quite similar to each other, unlike what was observed in the case of 2×*PDR3* and *pdr1*Δ. It is clear that Pdr1, even at a supposedly higher dosage, cannot activate the expression of *PDR5-yEGFP* more than half as well as the intact network. In fact, it may be that this limited activation strength of Pdr1 is the reason behind the resemblance in the dynamics of *PDR5-yEGFP* expression of 2×*PDR1* and *pdr3*Δ strains. It appears that maximum activation is achieved after the initial rise in the level of Pdr5-yEGFP.

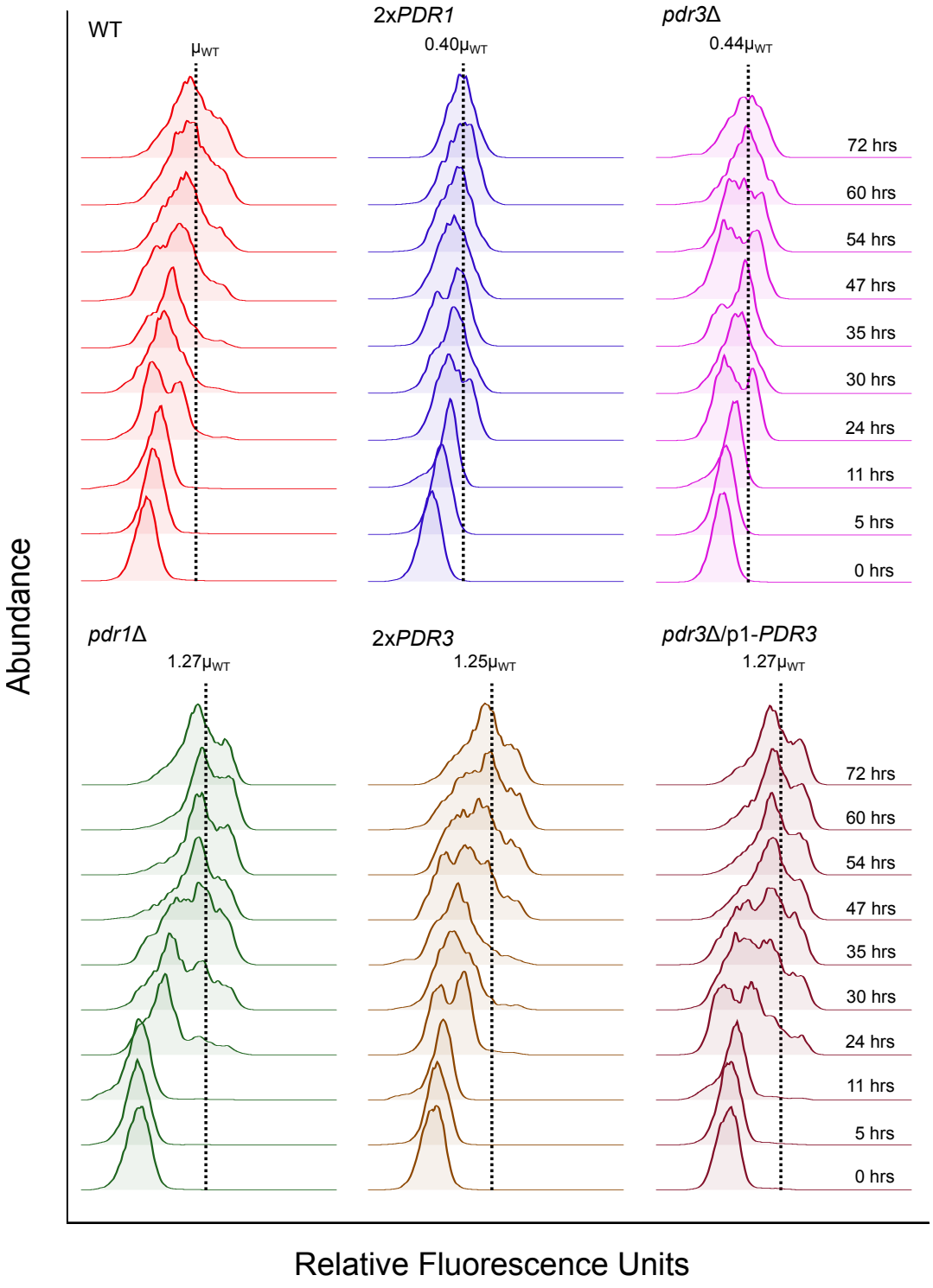

Figure 3.13: Flow cytometry analysis of mutants which contain one of the two TFs in various network configurations. The shift in the level of Pdr5-yEGFP in WT (red), 2×*PDR1* (dark blue), *pdr3*Δ (magenta), *pdr1*Δ (green), 2×*PDR3* (brown), and *pdr3*Δ/p1-*PDR3* (garnet) populations. This shift occurs with varying dynamics among these strains and yields different steady-state levels of Pdr5-yEGFP at the end of a 72-hour treatment with 0.1 μg/mL cycloheximide. Dashed lines indicate the mean level of Pdr5-yEGFP fluorescence for the last time point, which is expressed as a multiple of the WT value.

As the evidence for higher activity of Pdr3 over Pdr1 accumulated, we decided to further investigate the properties of these TFs by somewhat removing the effects of the network architecture. Therefore, we created strains in which one native TF was knocked out and the other was replaced by the first one (Figure 3.12B). The strain *pdr1*Δ/p3-*PDR1* was obtained by knocking out the native *PDR1* gene in the 2×*PDR1* strain using a *URA3* expression cassette, which left only the *PDR1* CDS driven from the pPDR3 promoter. Similarly, *pdr3*Δ/p1-*PDR3* was created by replacing the native *PDR3* gene with the *URA3* expression cassette keeping only one copy of *PDR3* controlled by the pPDR1. Selection of positive transformants and confirmation of correct transformation was performed as before.

For the *pdr1*Δ/p3-*PDR1* strain, the expression profile before drug treatment, its evolution during cycloheximide exposure, and the associated loss of viability were practically indistinguishable from that of *pdr1*Δ*pdr3*Δ mutants. Evidently, Pdr1 is not able to establish a basal level of Pdr5-yEGFP, when driven from the pPDR3 promoter, nor can it increase this protein's levels after addition of cycloheximide.

The other strain, however, strongly activates the expression of *PDR5-yEGFP* while cells grow in rich media, as anticipated. Moreover, the Pdr5-yEGFP profile of *pdr3*Δ/p1-*PDR3* cells evolved over time in a similar fashion to that of 2×*PDR3*, especially during the initial hours of cycloheximide treatment (Figure 3.13). Unlike the *pdr1*Δ strain, *pdr3*Δ/p1-*PDR3* cells demonstrated a more gradual elevation in the level of Pdr5-yEGFP at first. Nonetheless, they reached a similar steady-state level of Pdr5-yEGFP to both of the other Pdr3-containing strains.

Chapter 4

Discussion

The PDR network of *S. cerevisiae* has been accepted to be the major determinant of MDR in this organism. Therefore, as the centre piece of PDR in *S. cerevisiae*, *PDR5* becomes a key player in this process. Add to this the established role of *PDR5* homologues in drug resistance of pathogenic fungi and cancer cells, and it becomes a most attractive candidate for the study of MDR. A large body of work has been produced for the past two decades about the mechanism of action of Pdr5, and its homologues, in the extrusion of structurally and functionally variable drugs and its genetic regulation in the large context of *S. cerevisiae* PDR. However, few researchers have studied the gene expression of *PDR5* in its own right, rather than a reporter for its regulators, let alone detailed investigation of its long-term dynamics. Furthermore, only a handful of studies have considered the expression of *PDR5* in individual cells. Therefore, it is important to understand the individual-level dynamics of *PDR5* expression, as a principal element in the survival of *S. cerevisiae* in realistic environments, if we are to truly understand the concept of non-genetic MDR.

4.1 *PDR5*-mediated Bet Hedging

Bet hedging is an evolutionarily stable strategy that arises from temporally variable environments which change unpredictably [49]. Therefore, one cannot consider a population's strategy to be bet hedging, with certainty, unless the evolutionary history of the organism, for an appropriate amount of time, is known. However, in the absence of controlled or known selective environments, one can deduce bet hedging by its characteristic properties. The main hallmark of this strategy—particularly in single-cell organisms—is risk spreading across an isogenic population of individuals to increase the overall fitness of the genotype over time. Accordingly, evolution of a bet hedging strategy can be postulated when: i) an isogenic population of cells exhibits distinct phenotypes, and ii) each phenotype confers differential fitness to the individual exhibiting it in different environments [54].

Drug resistance is a case where bet hedging could be a useful strategy. On one hand, evidence for stochastic expression of general stress response elements, including drug resistance, in a variety of organisms is ubiquitous [21, 30, 37, 57]. On the other hand, noisy gene expression has been shown to be metabolically costly for cells, which is why mechanisms have been set in place to minimize the amount of noise in essential and housekeeping genes [29, 156, 157]. Moreover, overexpression of drug resistance genes has been specifically linked to reduced fitness in cells [33]. As such, bet hedging has been proposed as a mechanism for drug resistance in bacteria on multiple occasions [63, 64]; however, it has not been mechanistically shown to be used in eukaryotic drug resistance.

PDR5 is an ideal candidate for involvement in eukaryotic bet hedging. It is one of the main drug resistance genes of *S. cerevisiae*; the network, regulating its expression, has been shown to improve cell-cell variability both theoretically and experimentally; and its mRNA levels fluctuate, indicating transcriptional heterogeneity in the population [127].

4.1.1 Variability in the Level of Pdr5

The first task is to demonstrate that the hypothesized variability in expression of *PDR5* leads to phenotypic states with distinct fitness characteristics in drug and no-drug conditions. Since presentation of the phenotype is facilitated by the protein, we tagged the Pdr5 protein with yEGFP at its C-terminal. To the extent of our knowledge, only a handful of groups have published tagging of *PDR5* with GFP—all C-terminally—none of which have reported any significant loss of function [116, 158–161]. We did not encounter any noticeable decrease in the number of colonies formed by yEGFP-tagged individuals compared to the parental strain. Therefore, we consider the strain containing Pdr5-yEGFP (WT) to be representative of the parental BY4741 strain in its drug resistance properties and overall fitness.

Furthermore, we used galactose as an exclusive carbon source. Growth in glucose leads to a high basal level of *PDR5* expression (Figure 3.2 and [116]), and sole use of fermentation could give rise to ρ^0 cells with drug-independent high expression of *PDR5*. Galactose, however, does not induce the expression of *PDR5* as strongly as glucose. Using galactose as a carbon source generally leads to a mixture of fermentative and aerobic metabolism by *S. cerevisiae* [162]. However, the parental strain we chose to study—BY4741—is derived from *S. cerevisiae* S288C strain, harbouring a *gal2-* deletion, which does not allow metabolization of galactose anaerobically. In fact, S288C cells have been shown to maintain their mitochondrial DNA in galactose [163].

The variability in the population of WT cells, in their log phase of growth in galactose, is displayed in the form of a small subpopulation of cells—HES—with a mean expression level several folds larger than the rest of the population. Both cycloheximide and nocodazole cause a strong shift in the mean levels of Pdr5-yEGFP of WT cells. We used 0.1 µg/mL cycloheximide because larger concentrations of this drug—as low as 1 µg/mL—led to strong growth inhibition and inability of the population to regain its viability after more than a

week. The HES forms only a small proportion of the total population, but its mean level is close to that of drug-treated samples. Further inspection of HES indicated that it is unlikely to be caused by a mutation, as populations derived from different colonies at different times revert back to the same original profile after being enriched for HES (Figure 3.3).

A possibility was raised earlier that this reversion to the original expression profile may be due to a much greater fitness of the LES cells allowing them to overwhelm the HES. Two lines of evidence argue against this notion. First, HES cells can grow reasonably well on rich media (Figure 3.4), even when they express *PDR5-yEGFP* at its highest observed level after drug treatment (Figure 3.6). Second, if growth rate of the HES were negligible, with the assumption that LES has the same ∼3-hour doubling time as the parental BY4741 in galactose [164], it would take ∼3 hours for the proportion of cells in HES to halve. With this half-life, the HES would reach 1% of the population after 17 hours only. This is in contrast to the approximately 40 hours it takes, experimentally, for HES to reach 1% of the population, and its calculated half-life of more than 10 hours. Therefore, it appears that while LES cells do overtake HES cells, complete inundation of the latter by the former does not occur. Nevertheless, it bears mentioning that, given some non-zero rate of growth for cells of the HES, the final profile can be arrived at without the need for them to switch from the high-expression state to the low-expression one. Single-cell experiments following the expression level of *PDR5-yEGFP* over time after drug removal are best suited for settling the particular question of state switching under these conditions.

These results argue for a bimodal expression of *PDR5*. The population profile of WT cells with respect to the levels of Pdr5-yEGFP shows a clear bimodal characteristic before drug administration and after its removal. This bimodality does not appear to be accompanied by bistability since HES does not persist for long, as the major subpopulation, after enrichment or drug removal (Figures 3.3 and 3.5). Studies with synthetic networks have substantiated the possibility of obtaining bimodality without bistability in genetic

networks with a positive FBL and a short-lived TF [95]. These properties fit well with at least one of the TFs regulating *PDR5* expression—Pdr3 is in a positive FBL and has a half life of ∼51 minutes [165].

Bimodality in the expression of any gene in a genetically uniform population is a categorical example of non-genetic heterogeneity. Not only two distinct subpopulations exist, cells can potentially move from one to the other and share the possibility of experiencing the woes and blessings of each expression state. Therefore, the first requirement for classification of *PDR5* expression pattern as bet hedging is present.

4.1.2 Fitness Disparity of HES and LES

As previously noted, mere existence of phenotypic variability in a population does not signify a bet hedging strategy in that population. There need be some meaningful difference in fitness between various phenotypes under distinct environmental conditions. *PDR5* transports tens, if not hundreds, of compounds across the membrane. Therefore, its presence can modulate the fitness of an individual in as many environments. In order to demonstrate differential growth dynamics of the two subpopulations of *S. cerevisiae* with regards to *PDR5* expression, we used two such environments—cycloheximide-containing and rich media.

The first clue for a potential difference in the fitness of the two subpopulations came from the observation that the HES distribution coincided quite well with that of drug-treated populations (with both cycloheximide and nocodazole in Figure 3.2). It stands to reason that if some cells already express a certain level of Pdr5-yEGFP required to survive in presence of these drugs, they would have a better chance of survival during drug treatment. Enrichment of populations for HES and LES, using FACS, allowed us to unequivocally demonstrate a clear difference in the fitness of these subpopulations in said environments. The spot assay experiment of Figure 3.3 simply and efficiently reveals

an unmistakeable disparity in the growth capabilities of populations enriched for HES and LES. Furthermore, the inability of LES-enriched samples to survive as well as HES-enriched samples, in addition to the slower growth of the unsorted sample itself, leads us to conclude that the increase in the mean level of Pdr5-yEGFP after cycloheximide treatment is not purely due to an induction of *PDR5* expression by its regulatory elements 'after' drug addition. The contribution of HES to the general survival and growth of the population as a whole, in the presence of cycloheximide, is not negligible.

However, if fitness of the HES were equal to that of the LES in the absence of drug, one would predict it to be the dominant phenotype since it increases the fitness of the population in presence of the drug. However, not only is the high expression of *PDR5* not the sole phenotype in these populations but, in fact, it is merely present in a very small fraction of cells. Thus, it would appear that high expression of *PDR5* is associated with some fitness cost when cells grow in rich media. Yet, it is entirely possible that the fitness defect of the HES in the absence of drug is not as severe as that of LES in its presence. In such a case, we may not be able to easily observe the difference in the growth rates. Indeed, the HES-enriched sample of the WT strain did show a slight growth defect on rich media plates although the incomplete enrichment of HES in the high-gated samples certainly obscured the fitness defect of the HES under these conditions. Therefore, we resorted to investigating HESs sorted from the bimodal populations obtained after drug treatment to obtain samples that were more enriched in high-expressing cells. While showing superior growth on cycloheximide-containing plates, these HES-enriched samples had an unambiguous growth deficiency when grown on rich media compared to LES-enriched samples. Furthermore, samples sorted for the HES of the *pdr1*Δ mutant were similar to the HES-enriched samples of WT in their growth deficiency on rich media.

If we combine the results from mean levels of Pdr5-yEGFP in these samples with the qualitative view of their growth deficiency in rich media, we arrive at a correlation between these two parameters. The levels of Pdr5-yEGFP are lower in the HES of WT than that of

*pdr1*Δ before drug treatment (Figure 3.7C); similarly, the HES levels of Pdr5-yEGFP in WT cells are consistently lower than those of *pdr1*Δ cells after drug treatment (compare Figure 3.5C with Figure 3.10B). Also, it is apparent that HES-enriched samples of the WT strain before drug treatment have the highest growth efficiency on rich media followed by HES-enriched samples of *pdr1*Δ cells before exposure to cycloheximide (Figures 3.4 and 3.8). Finally, WT HES samples grow better than *pdr1*Δ HES samples that are sorted after cycloheximide treatment (Figure 3.6). In summary, for ability of HES to grow in rich media: WT before drug > *pdr1*Δ before drug > WT after drug > *pdr1*Δ after drug; for mean level of Pdr5-yEGFP in HES cells: WT before drug < *pdr1*Δ before drug < WT after drug < *pdr1*Δ after drug. These results suggest that higher levels of Pdr5-yEGFP decrease the fitness of cells when grown without drug. An inverse relationship between higher levels of Pdr5-yEGFP and growth in the absence of drug is in agreement with available evidence. In a recent study, transmembrane proteins were identified as one of two categories of proteins to have an observable impact on fitness when overexpressed [166]. Furthermore, the seemingly idiosyncratically constitutive ATP hydrolysis by Pdr5 [115] can become prohibitive to the growth of an individual when it is expressed at high levels.

4.2 Transcriptional Regulation of *PDR5*

Recognizing that *PDR5* could be a part of a bet hedging strategy by *S. cerevisiae* directed our attention to understanding how this strategy is implemented across the population. Based on the evidence presented in the Introduction, the intricate network regulating *PDR5* expression seemed the most likely reason behind implementation of this strategy. We tackled the question of *PDR5* transcriptional regulation through construction of variants of the *PDR5* regulatory network with strains containing only one of its two major transcriptional activators in a number of configurations.

4.2.1 Peculiar Behaviour of Pdr1 and Pdr3

Both *PDR1* and *PDR3* were discovered by genetic mapping of *S. cerevisiae* mutations that caused resistance to two or more unrelated drugs [121, 167]. The sequence homology and overlap in targets for these two TFs, as well as the ability of cells to survive on drugs in absence of one or the other, led many researchers to conclude that their functions are largely redundant. Furthermore, identifying Pdr1 as a regulator of *PDR3* expression resulted in the belief that Pdr1 is the master regulator of PDR, while Pdr3 only plays a secondary part in this process [168]. This belief has been somewhat challenged since the Pdr1-independent role of Pdr3 in activating a large number of genes—including *PDR5*—in ρ^0 cells was elucidated. Yet, the general attitude in *S. cerevisiae* PDR literature is to consider Pdr3 as the less important factor in drug resistance.

Based on the overall literature review conducted at the beginning of this study, we expected that deletion mutants lacking *pdr3* would fair relatively well, while those without *pdr1* would suffer more. However, from our first experiments, this expectation was not met. Cells of the *pdr1*Δ strain bearing only the *PDR3* gene, not only had a similar basal expression level to that of both *pdr3*Δ and WT strains but also possessed an HES with a higher mean level of Pdr5-yEGFP than that of WT (Figure 3.7). The level of Pdr3 has been estimated to be an order of magnitude lower than that of Pdr1 under standard growth conditions [137]. However, these estimates were obtained from high-throughput collections of data and do not take into account mutations or changes in growth conditions. Despite their homology and hypothesized redundancy, Pdr1 and Pdr3 have many targets and functions that are distinct from one another. Furthermore, the role of Pdr3 in response to loss of mitochondrial DNA hints at Pdr1-independent regulation of this TF. Therefore, it is likely that in the absence of Pdr1, a compensatory mechanism upregulates Pdr3 leading to the observed basal activation of *PDR5* in the *pdr1*Δ strain. We initially considered this to be the most likely scenario; however, the phenotype of *pdr1*Δ after drug treatment

forced us to reconsider.

Cycloheximide treatment of *pdr1*Δ cells resulted in mean levels of Pdr5-yEGFP nearly two fold larger than those of WT cells at steady state (Figure 3.9). These results were unpredicted in that they suggested stronger activity of Pdr3 than Pdr1. These two TFs have been shown to form homo and heterodimers *in vivo* [134]. Therefore, the most parsimonious explanation for this behaviour is that Pdr3 can better activate *PDR5*, and Pdr1 attenuates its activity in WT cells by binding to it. A potential reason for the lower activity of Pdr1 is the presence of an inhibitory domain about 250 amino acids from its N terminal [169]. While overexpression of Pdr1 has been implicated in repression of some genes [143], the specific function of this domain has not yet been established. Moreover, this domain is conserved in most TFs of the Gal4 family [170], including Pdr3. In fact, Pdr1 and Pdr3 share high homology in the two main motifs of this domain [131]. In contrast, they do not share as much homology in their activation domains [171]. Therefore, it is possible that the difference in the activities of these TFs is due to variation in their activation domains.

It must also be noted that a higher level of Pdr5-yEGFP in *pdr1*Δ cells was not specific to cycloheximide, but was also observed in presence of nocodazole. To our knowledge, no published work has claimed that Pdr3 activates *PDR5* more strongly than Pdr1. The only source to corroborate our findings is a PhD thesis [172], in which *pdr1*Δ cells were shown to grow better on cycloheximide media than *pdr3*Δ cells. We confirmed these results, and the fact that they were not published, with the thesis supervisor—Dr. Turcotte, McGill University—through personal communication. The lack of support for this claim within the literature is not particularly surprising. The large majority of studies we have examined focus on the immediate to short-term response of Pdr5 levels—or its mRNA—to the presence or absence of either TF. In fact, we have not come across any studies, which have considered the dynamical change in the levels of Pdr5 over a timescale longer than one day. Interestingly, our results indicate that the effect of higher Pdr3 activity on Pdr5

levels does not become apparent for at least the first 12 hours of growth, and this effect on cell survival does not become evident until ∼30 hours after treatment (Figure 3.9). Therefore, the higher activity of Pdr3 could easily be overlooked in short-term studies.

Another clue to the higher activity of Pdr3 comes from the other mutants generated in our study. The bottom panel of Figure 3.13 shows flow cytometry histograms for three mutants that contained Pdr3 as the only TF to activate *PDR5*. Regardless of the regulatory network architecture containing the TF(s)—positive FBL in *pdr1*Δ, C1FFL with embedded positive FBL in 2×*PDR3*, and direct activation in *pdr3*Δ/p1-*PDR3*—all these strains reached a very similar steady state level of Pdr5-yEGFP at the end of cycloheximide treatment. We observed an analogous situation in the mutants containing only Pdr1 as their activator. Together, these results implicate that, at the height of cycloheximide treatment, the promoter of *PDR5* is saturated with present TFs. Furthermore, the expression of *PDR5* is activated more strongly by Pdr3 homodimers than Pdr1 homodimers, with the activity of heterodimers being intermediate. Moreover, cold competition assays have shown that cycloheximide binds Pdr3 with an approximately three fold less affinity than it does Pdr1 [138], implying that Pdr3 may not need cycloheximide binding for its activity as much as Pdr1 does.

4.2.2 The Role of the Network Architecture

The *PDR5* regulatory network contains two main motifs, both of which are theorized to increase variability in target expression. Therefore, it is natural to presume that these features are instrumental in the establishment of expression variability noticed in the levels of *PDR5*. Our aim was to study each motif separately from the other and compare it to the case of direct activation. However, it was impossible for us to generate C1FFL alone. There are two potential ways to destroy the positive FBL in the network—either by removing the binding sites for Pdr3 on its own promoter or by mutating its DNA binding domain.

Due to the special regulatory overlap between paralogous Pdr1 and Pdr3—they bind the same PDREs—we were not able to take either of these approaches. The first would have abolished Pdr1 activation of *PDR3* and the second would have removed Pdr3 activation of *PDR5*. Therefore, we resorted to the study of direct activation, positive FBL, and the C1FFL-FBL combination.

With regards to promotion of variability and generation of an easily identified HES, the *pdr1*Δ strain containing only the positive FBL behaved as expected. The two subpopulations of *pdr1*Δ reveal a markedly more disjoint character than those of the WT strain before addition of the drug, during treatment, and after its removal (Figures 3.7 and 3.10). All of these characteristics are consistent with those predicted from a positive FBL. Yet, the WT strain contains this same positive FBL; therefore, the less distinct separation between its subpopulations must be due to the action of direct activation from Pdr1. The WT LES has a higher mean level of Pdr5-yEGFP than *pdr1*Δ LES, while its HES has a smaller mean level than that of *pdr1*Δ. Therefore, it may be that the lower activity of Pdr1 contributes to the reduced HES of WT. At the same time, the higher concentration of Pdr1 results in increasing the level of WT LES—which is similar to that of *pdr3*Δ in its distribution.

In addition, the importance of the C1FFL in the regulation of *PDR5* becomes less clear, based on our results. Pdr3 activates the expression of *PDR5* in the absence of Pdr1 to about 80% of WT basal levels. Hence, regulation of this gene by Pdr1 and Pdr3 is not additive, and the *PDR1* $\longrightarrow$ *PDR3* edge of the network is not essential for Pdr3-mediated activation of *PDR5*. The two network variants generated with a C1FFL-FBL architecture, which featured either Pdr1 or Pdr3 in both activation positions, support this notion. Figure 3.13 shows that, at least on a qualitative level, both of these C1FFL networks—2$\times$*PDR3* and 2$\times$*PDR1*—behave similarly to their direct-activation counterparts—*pdr3*Δ/p1-*PDR3* and *pdr3*Δ, respectively. In fact, the only difference between the five strains featuring a direct-activation edge—including WT itself—with *pdr1*Δ is their initially gradual increase in

levels of Pdr5-yEGFP, as opposed to the latter's sharp jump. Therefore, it seems that the direct activation edge—$X \longrightarrow PDR5$—acts to initially absorb the shock of drug treatment and enhance survival by gradually increasing the level of *PDR5*. This mechanism may be beneficial in maximizing survival in short-lived encounters with xenobiotics without the need for the full activation of the network.

Chapter 5

Conclusion

We have provided evidence indicating that the expression of *PDR5* forms a basis for a bet hedging strategy in the drug resistance response of *S. cerevisiae*. To explain this phenomenon, we propose a model describing the role of *PDR5* regulation in giving rise to this strategy. The positive FBL of Pdr3 leads to a bimodal expression profile of *PDR5*, which results in generation of two subpopulations—one with high levels of Pdr5 and one with low levels. The higher levels of Pdr5 allow for the survival of cells exposed to toxic xenobiotics, especially cycloheximide, while decreasing their fitness during growth in optimal conditions. In contrast, cells with lower levels of Pdr5 grow maximally in rich media, but suffer when xenobiotics are present. The proportion of the HES is kept at a much lower level than LES, presumably due to reduced fitness in optimal growth conditions. Populations in which this balance has been perturbed re-establish this proportion after some time indicating that it may constitute a dynamically maintained steady state, in which cells stochastically transition back and forth between low and high expression. Pdr1 appears to be a weaker TF, while being expressed at a higher level, than Pdr3 and attenuates its activity when present. We postulate that this disparity in the activation strength of Pdr1 and Pdr3 keeps the proportion of HES in check. This function may have evolved during the evolutionary history of *S. cerevisiae* to fine tune the proportion of HES to LES

according to the approximate frequency of toxin exposure. However, it must be kept in mind that Pdr1 and Pdr3 regulate the expression of a large number of genes, either in concert or individually. Therefore, their relative activity will have been selected for by the phenotypic consequences of their regulation of these targets, too. Nonetheless, our analysis would remain largely valid for their other targets since most of them are involved in response to drugs and other stress conditions, and their expression cost and benefit would broadly resemble that of *PDR5*. Furthermore, the presence of a route for direct activation of *PDR5* appears to enable *S. cerevisiae* cells to respond rapidly to xenobiotic exposure. However, we could not find a direct link between the specific C1FFL architecture and the bet hedging strategy in this instance. Lastly, given our results and those reported in the literature, we expect that regulation of *PDR5* follows a complex pattern based on a bet hedging strategy, but enhanced through increase of TF activity by direct binding to the drug. Such an integrated regulation scheme is most appropriate when responding to novel xenobiotic challenges, as well as those previously encountered.

Many questions remain to be answered, and some inconsistencies ought to be addressed. We have speculated, based on genetic perturbation data, that Pdr3 is a stronger activator than Pdr1. However, this approach does not account for changes in upstream or downstream effectors of either factor upon deletion of the other. Therefore, their individual and combined DNA binding affinities, along with their homodimeric and heterodimeric activities should be explored in physiochemical detail to confirm these results. Furthermore, this apparent difference in activities may be due to their differential affinities to PDRE variants on the *PDR5* promoter. A systematic investigation of these binding elements would be valuable in understanding the significance of PDRE variants and their specific positioning in establishing the *PDR5* expression profile. Additionally, the ambiguity in regulation of *PDR1* and the Pdr1-independent control of *PDR3* expression, confound our results. For example, the complex positive FBL created by *PDR1*/*PDR3* and *RPN4*, compromises the notion of 'direct activation' from the pPDR1 promoter. We have, in fact, observed surpris-

ing appearance of an HES in the profile of *pdr3*Δ/p1-*PDR3* cells. This is inconsistent with the expected loss of Pdr3-mediated feedback, and should be further examined. If *RPN4* proves to form this positive FBL, under optimal conditions, it would lend more support to the notion of a weaker Pdr1 since no HES was observed in *pdr3*Δ cells. However, it would require us to adjust our model to include the additional regulatory input. Apart from the intrigue of *RPN4*, a number of other exploratory avenues could be pursued. Many of the recently identified modulators of *PDR5* activity—found using synthetic genetic array technology—directly point to general transcriptional regulators—such as SAGA and the Mediator complex, among others—which interact variably with Pdr1 and Pdr3. These interactions could form a basis for the apparent difference in the strength of their activity, and fine tuning of subpopulation proportions. This knowledge could be exploited to understand the molecular mechanism used for defining these proportions. Finally, *PDR5* is not the only target of Pdr1/Pdr3; thus, an investigation of expression profiles of some of their other targets would shed light on the extent of their involvement in the *S. cerevisiae* bet hedging strategy. We hope that this first demonstration of a eukaryotic bet hedging strategy against toxin exposure, especially involving an important class of proteins mediating MDR, would pave the way for its identification in other systems.

References

[1] Nathan, C. (2004) Antibiotics at the crossroads. *Nat Cell Biol* **431**, 899–902.

[2] Davies, J. (1996) Bacteria on the rampage. *Nature* **383**, 219–220.

[3] Longley, D. B & Johnston, P. G. (2005) Molecular mechanisms of drug resistance. *J Pathol* **205**, 275–292.

[4] Walsh, C. (2000) Molecular mechanisms that confer antibacterial drug resistance. *Nature* **406**, 775–781.

[5] Varghese, J. N, Smith, P. W, Sollis, S. L, Blick, T. J, Sahasrabudhe, A, McKimm-Breschkin, J. L, & Colman, P. M. (1998) Drug design against a shifting target: a structural basis for resistance to inhibitors in a variant of influenza virus neuraminidase. *Structure* **6**, 735–746.

[6] Andersson, D. I. (2003) Persistence of antibiotic resistant bacteria. *Curr Opin Microbiol* **6**, 452–456.

[7] White, T. C, Marr, K. A, & Bowden, R. A. (1998) Clinical, cellular, and molecular factors that contribute to antifungal drug resistance. *Clin Microbiol Rev* **11**, 382–402.

[8] Zhang, Y, Cheng, Y, Zhang, L, Ren, X, Huber-Keener, K. J, Lee, S, Yun, J, Wang, H.-G, & Yang, J.-M. (2011) Inhibition of eEF-2 kinase sensitizes human glioma cells to TRAIL and down-regulates Bcl-xL expression. *Biochem Biophys Res Commun* **414**, 129–134.

[9] Sharma, S. V, Lee, D. Y, Li, B, Quinlan, M. P, Takahashi, F, Maheswaran, S, McDermott, U, Azizian, N, Zou, L, Fischbach, M. A, Wong, K.-K, Brandstetter, K, Wittner, B, Ramaswamy, S, Classon, M, & Settleman, J. (2010) A chromatin-mediated reversible drug-tolerant state in cancer cell subpopulations. *Cell* **141**, 69–80.

[10] Drake, J. W, Charlesworth, B, Charlesworth, D, & Crow, J. F. (1998) Rates of spontaneous mutation. *Genetics* **148**, 1667–1686.

[11] Cirz, R. T, Chin, J. K, Andes, D. R, de Crécy-Lagard, V, Craig, W. A, & Romesberg, F. E. (2005) Inhibition of mutation and combating the evolution of antibiotic resistance. *PLoS Biol* **3**, e176–e176.

[12] Bjedov, I, Tenaillon, O, Gérard, B, Souza, V, Denamur, E, Radman, M, Taddei, F, & Matic, I. (2003) Stress-induced mutagenesis in bacteria. *Science* **300**, 1404–1409.

[13] Bindra, R. S & Glazer, P. M. (2007) Co-repression of mismatch repair gene expression by hypoxia in cancer cells: role of the Myc/Max network. *Cancer Lett* **252**, 93–103.

[14] Woodford, N & Ellington, M. J. (2007) The emergence of antibiotic resistance by mutation. *Clin Microbiol Infect* **13**, 5–18.

[15] Kumar, R, Chaudhary, K, Gupta, S, Singh, H, Kumar, S, Gautam, A, Kapoor, P, & Raghava, G. P. S. (2013) CancerDR: Cancer drug resistance database. *Sci Rep* **3**, 1445.

[16] Marusyk, A, Almendro, V, & Polyak, K. (2012) Intra-tumour heterogeneity: a looking glass for cancer? *Nat Rev Cancer* **12**, 323–334.

[17] Kreso, A, O'Brien, C. A, van Galen, P, Gan, O. I, Notta, F, Brown, A. M. K, Ng, K, Ma, J, Wienholds, E, Dunant, C, Pollett, A, Gallinger, S, McPherson, J, Mullighan, C. G, Shibata, D, & Dick, J. E. (2013) Variable clonal repopulation dynamics influence chemotherapy response in colorectal cancer. *Science* **339**, 543–548.

[18] Brock, A, Chang, H, & Huang, S. (2009) Non-genetic heterogeneity–a mutation-independent driving force for the somatic evolution of tumours. *Nat Rev Genet* **10**, 336–342.

[19] Deris, J. B, Kim, M, Zhang, Z, Okano, H, Hermsen, R, Groisman, A, & Hwa, T. (2013) The innate growth bistability and fitness landscapes of antibiotic-resistant bacteria. *Science* **342**, 1237435.

[20] Kint, C. I, Verstraeten, N, Fauvart, M, & Michiels, J. (2012) New-found fundamentals of bacterial persistence. *Trends Microbiol* **20**, 577–585.

[21] Niepel, M, Spencer, S. L, & Sorger, P. K. (2009) Non-genetic cell-to-cell variability and the consequences for pharmacology. *Curr Opin Chem Biol* **13**, 556–561.

[22] Rotem, E, Loinger, A, Ronin, I, Levin-Reisman, I, Gabay, C, Shoresh, N, Biham, O, & Balaban, N. Q. (2010) Regulation of phenotypic variability by a threshold-based mechanism underlies bacterial persistence. *Proc Natl Acad Sci USA* **107**, 12541–12546.

[23] Charlebois, D. A & Kærn, M. (2012) What all the noise is about: The physical basis of cellular individuality. *Can J Phys* **90**, 919–923.

[24] Kaern, M, Elston, T. C, Blake, W. J, & Collins, J. J. (2005) Stochasticity in gene expression: from theories to phenotypes. *Nat Rev Genet* **6**, 451–464.

[25] Raj, A, Peskin, C. S, Tranchina, D, Vargas, D. Y, & Tyagi, S. (2006) Stochastic mRNA synthesis in mammalian cells. *PLoS Biol* **4**, e309.

[26] Cox, C. D, McCollum, J. M, Allen, M. S, Dar, R. D, & Simpson, M. L. (2008) Using noise to probe and characterize gene circuits. *Proc Natl Acad Sci USA* **105**, 10809–10814.

[27] Eldar, A & Elowitz, M. B. (2010) Functional roles for noise in genetic circuits. *Nature* **467**, 167–173.

[28] Sumner, E. R & Avery, S. V. (2002) Phenotypic heterogeneity: Differential stress resistance among individual cells of the yeast Saccharomyces cerevisiae. *Microbiology* **148**, 345–351.

[29] Raj, A & van Oudenaarden, A. (2008) Nature, nurture, or chance: stochastic gene expression and its consequences. *Cell* **135**, 216–226.

[30] Locke, J. C. W, Young, J. W, Fontes, M, Hernández Jiménez, M. J, & Elowitz, M. B. (2011) Stochastic pulse regulation in bacterial stress response. *Science* **334**, 366–369.

[31] Poole, K. (2012) Bacterial stress responses as determinants of antimicrobial resistance. *J Antimicrob Chemother* **67**, 2069–2089.

[32] Blake, W. J, Balázsi, G, Kohanski, M. A, Isaacs, F. J, Murphy, K. F, Kuang, Y, Cantor, C. R, Walt, D. R, & Collins, J. J. (2006) Phenotypic consequences of promoter-mediated transcriptional noise. *Mol Cell* **24**, 853–865.

[33] Nevozhay, D, Adams, R. M, Van Itallie, E, Bennett, M. R, & Balázsi, G. (2012) Mapping the environmental fitness landscape of a synthetic gene circuit. *PLoS Comput Biol* **8**, e1002480.

[34] Korch, S. B, Henderson, T. A, & Hill, T. M. (2003) Characterization of the hipA7 allele of Escherichia coli and evidence that high persistence is governed by (p)ppGpp synthesis. *Mol Microbiol* **50**, 1199–1213.

[35] Levchenko, A, Mehta, B. M, Niu, X, Kang, G, Villafania, L, Way, D, Polycarpe, D, Sadelain, M, & Larson, S. M. (2005) Intercellular transfer of P-glycoprotein mediates acquired multidrug resistance in tumor cells. *Proc Natl Acad Sci USA* **102**, 1933–1938.

[36] Misra, S, Ghatak, S, & Toole, B. P. (2005) Regulation of MDR1 expression and drug resistance by a positive feedback loop involving hyaluronan, phosphoinositide 3-kinase, and ErbB2. *J Biol Chem* **280**, 20310–20315.

[37] Cohen, A. A, Geva-Zatorsky, N, Eden, E, Frenkel-Morgenstern, M, Issaeva, I, Sigal, A, Milo, R, Cohen-Saidon, C, Liron, Y, Kam, Z, Cohen, L, Danon, T, Perzov, N, & Alon, U. (2008) Dynamic Proteomics of Individual Cancer Cells in Response to a Drug. *Science* **322**, 1511–1516.

[38] Menu, F, Roebuck, J. P, & Viala, M. (2000) Bet-hedging diapause strategies in stochastic environments. *Am Nat* **155**, 724–734.

[39] Sozou, P. D & Kirkwood, T. B. (2001) A stochastic model of cell replicative senescence based on telomere shortening, oxidative stress, and somatic mutations in nuclear and mitochondrial DNA. *J Theor Biol* **213**, 573–586.

[40] Thattai, M & van Oudenaarden, A. (2004) Stochastic gene expression in fluctuating environments. *Genetics* **167**, 523–530.

[41] Zhuravel, D, Fraser, D, St-Pierre, S, Tepliakova, L, Pang, W. L, Hasty, J, & Kaern, M. (2010) Phenotypic impact of regulatory noise in cellular stress-response pathways. *Syst Synth Biol* **4**, 105–116.

[42] Gupta, P. B, Fillmore, C. M, Jiang, G, Shapira, S. D, Tao, K, Kuperwasser, C, & Lander, E. S. (2011) Stochastic state transitions give rise to phenotypic equilibrium in populations of cancer cells. *Cell* **146**, 633–644.

[43] Charlebois, D. A, Abdennur, N, & Kaern, M. (2011) Gene expression noise facilitates adaptation and drug resistance independently of mutation. *Phys Rev Lett* **107**, 218101.

[44] Cohen, D. (1966) Optimizing reproduction in a randomly varying environment. *J Theor Biol* **12**, 119–129.

[45] Gillespie, J. H. (1974) Nautural selection for within-generation variance in offspring number. *Genetics* **76**, 601–606.

[46] Slatkin, M. (1974) Hedging one's evolutionary bets. *Nature* **250**, 704–705.

[47] Dempster, E. R. (1955) Maintenance of genetic heterogeneity. *Cold Spring Harb Symp Quant Biol* **20**, 25–32.

[48] Orr, H. A. (2009) Fitness and its role in evolutionary genetics. *Nat Rev Genet* **10**, 531–539.

[49] Seger, J & Brockmann, H. J. (1987) in *Oxford Surveys in Evolutionary Biology*, eds. Harvey, P. H & Partridge, L. (Oxford University Press, Oxford), pp. 182–211.

[50] Stearns, S. C. (1976) Life-history tactics: a review of the ideas. *Q Rev Biol* **51**, 3–47.

[51] Rees, M, Jessica, C, Metcalf, E, & Childs, D. Z. (2010) Bet-hedging as an evolutionary game: the trade-off between egg size and number. *Proc Biol Sci* **277**, 1149–1151.

[52] Mountford, M. D. (1971) Population survival in a variable environment. *J Theor Biol* **32**, 75–79.

[53] Simons, A. M. (2011) *Modes of response to environmental change and the elusive empirical evidence for bet hedging.* pp. 1601–1609.

[54] De Jong, I. G, Haccou, P, & Kuipers, O. P. (2011) Bet hedging or not? A guide to proper classification of microbial survival strategies. *BioEssays* **33**, 215–223.

[55] Stumpf, M. P. H, Laidlaw, Z, & Jansen, V. A. A. (2002) Herpes viruses hedge their bets. *Proc Natl Acad Sci USA* **99**, 15234–15237.

[56] Newby, G. A & Lindquist, S. (2013) Blessings in disguise: biological benefits of prion-like mechanisms. *Trends Cell Biol* **23**, 251–259.

[57] Fraser, D & Kaern, M. (2009) A chance at survival: gene expression noise and phenotypic diversification strategies. *Mol Microbiol* **71**, 1333–1340.

[58] Beaumont, H. J. E, Gallie, J, Kost, C, Ferguson, G. C, & Rainey, P. B. (2009) Experimental evolution of bet hedging. *Nature* **462**, 90–93.

[59] Müller, J, Hense, B. A, Fuchs, T. M, Utz, M, & Pötzsche, C. (2013) Bet-hedging in stochastically switching environments. *J Theor Biol* **336**, 144–157.

[60] King, O. D & Masel, J. (2007) The evolution of bet-hedging adaptations to rare scenarios. *Theor Popul Biol* **72**, 560–575.

[61] Tsuru, S, Yasuda, N, Murakami, Y, Ushioda, J, Kashiwagi, A, Suzuki, S, Mori, K, Ying, B.-W, & Yomo, T. (2011) Adaptation by stochastic switching of a monostable genetic circuit in Escherichia coli. *Mol Syst Biol* **7**, 493.

[62] Wolf, D. M, Vazirani, V. V, & Arkin, A. P. (2005) Diversity in times of adversity: probabilistic strategies in microbial survival games. *J Theor Biol* **234**, 227–253.

[63] Garcia-Bernardo, J & Dunlop, M. J. (2013) Tunable stochastic pulsing in the Escherichia coli multiple antibiotic resistance network from interlinked positive and negative feedback loops. *PLoS Comput Biol* **9**, e1003229.

[64] Veening, J.-W, Smits, W. K, & Kuipers, O. P. (2008) Bistability, epigenetics, and bet-hedging in bacteria. *Annu Rev Microbiol* **62**, 193–210.

[65] van der Woude, M, Braaten, B, & Low, D. (1996) Epigenetic phase variation of the pap operon in Escherichia coli. *Trends Microbiol* **4**, 5–9.

[66] Silverblatt, F. J, Dreyer, J. S, & Schauer, S. (1979) Effect of pili on susceptibility of Escherichia coli to phagocytosis. *Infect Immun* **24**, 218–223.

[67] Sureka, K, Ghosh, B, Dasgupta, A, Basu, J, Kundu, M, & Bose, I. (2008) Positive feedback and noise activate the stringent response regulator rel in mycobacteria. *PLoS ONE* **3**, e1771.

[68] Veening, J.-W, Stewart, E. J, Berngruber, T. W, Taddei, F, Kuipers, O. P, & Hamoen, L. W. (2008) Bet-hedging and epigenetic inheritance in bacterial cell development. *Proc Natl Acad Sci USA* **105**, 4393–4398.

[69] Acar, M, Mettetal, J. T, & van Oudenaarden, A. (2008) Stochastic switching as a survival strategy in fluctuating environments. *Nat Genet* **40**, 471–475.

[70] Graham, J. K, Smith, M. L, & Simons, A. M. (2014) Experimental evolution of bet hedging under manipulated environmental uncertainty in Neurospora crassa. *Proc Biol Sci* **281**.

[71] Fudenberg, D & Imhof, L. A. (2012) Phenotype switching and mutations in random environments. *Bull Math Biol* **74**, 399–421.

[72] Levy, S. F, Ziv, N, & Siegal, M. L. (2012) Bet hedging in yeast by heterogeneous, age-correlated expression of a stress protectant. *PLoS Biol* **10**, e1001325.

[73] Milo, R, Shen-Orr, S, Itzkovitz, S, Kashtan, N, Chklovskii, D, & Alon, U. (2002) Network motifs: simple building blocks of complex networks. *Science* **298**, 824–827.

[74] Lee, T. I, Rinaldi, N. J, Robert, F, Odom, D. T, Bar-Joseph, Z, Gerber, G. K, Hannett, N. M, Harbison, C. T, Thompson, C. M, Simon, I, Zeitlinger, J, Jennings, E. G, Murray, H. L, Gordon, D. B, Ren, B, Wyrick, J. J, Tagne, J.-B, Volkert, T. L, Fraenkel, E, Gifford, D. K, & Young, R. A. (2002) Transcriptional regulatory networks in Saccharomyces cerevisiae. *Science* **298**, 799–804.

[75] Alon, U. (2007) Network motifs: theory and experimental approaches. *Nat Rev Genet* **8**, 450–461.

[76] Thomas, R, Thieffry, D, & Kaufman, M. (1995) Dynamical behaviour of biological regulatory networks–I. Biological role of feedback loops and practical use of the concept of the loop-characteristic state. *Bull Math Biol* **57**, 247–276.

[77] Mangan, S & Alon, U. (2003) Structure and function of the feed-forward loop network motif. *Proc Natl Acad Sci USA* **100**, 11980–11985.

[78] Shoval, O & Alon, U. (2010) SnapShot: network motifs. *Cell* **143**, 326–e1.

[79] Mangan, S, Itzkovitz, S, Zaslaver, A, & Alon, U. (2006) The incoherent feed-forward loop accelerates the response-time of the gal system of Escherichia coli. *J Mol Biol* **356**, 1073–1081.

[80] Mangan, S, Zaslaver, A, & Alon, U. (2003) The coherent feedforward loop serves as a sign-sensitive delay element in transcription networks. *J Mol Biol* **334**, 197–204.

[81] Goentoro, L, Shoval, O, Kirschner, M. W, & Alon, U. (2009) The incoherent feed-forward loop can provide fold-change detection in gene regulation. *Mol Cell* **36**, 894–899.

[82] Kim, J, Khetarpal, I, Sen, S, & Murray, R. M. (2014) Synthetic circuit for exact adaptation and fold-change detection. *Nucleic Acids Res*.

[83] Kittisopikul, M & Süel, G. M. (2010) Biological role of noise encoded in a genetic network motif. *Proc Natl Acad Sci USA* **107**, 13300–13305.

[84] Shahrezaei, V, Ollivier, J. F, & Swain, P. S. (2008) Colored extrinsic fluctuations and stochastic gene expression. *Mol Syst Biol* **4**, 196.

[85] Miller, J. G. (1965) Living systems: Basic concepts. *Syst Res* **10**, 193–237.

[86] Rosenfeld, N, Elowitz, M. B, & Alon, U. (2002) Negative autoregulation speeds the response times of transcription networks. *J Mol Biol* **323**, 785–793.

[87] Rao, C. V, Wolf, D. M, & Arkin, A. P. (2002) Control, exploitation and tolerance of intracellular noise. *Nature* **420**, 231–237.

[88] Arias, A. M & Hayward, P. (2006) Filtering transcriptional noise during development: concepts and mechanisms. *Nat Rev Genet* **7**, 34–44.

[89] Becskei, A & Serrano, L. (2000) Engineering stability in gene networks by autoregulation. *Nature* **405**, 590–593.

[90] Nevozhay, D, Adams, R. M, Murphy, K. F, Josic, K, & Balázsi, G. (2009) Negative autoregulation linearizes the dose-response and suppresses the heterogeneity of gene expression. *Proc Natl Acad Sci USA* **106**, 5123–5128.

[91] Chalancon, G, Ravarani, C. N. J, Balaji, S, Martinez-Arias, A, Aravind, L, Jothi, R, & Babu, M. M. (2012) Interplay between gene expression noise and regulatory network architecture. *Trends Genet* **28**, 221–232.

[92] Maamar, H & Dubnau, D. (2005) Bistability in the Bacillus subtilis K-state (competence) system requires a positive feedback loop. *Mol Microbiol* **56**, 615–624.

[93] Acar, M, Becskei, A, & van Oudenaarden, A. (2005) Enhancement of cellular memory by reducing stochastic transitions. *Nature* **435**, 228–232.

[94] Nicol-Benoît, F, Le-Goff, P, Le-Dréan, Y, Demay, F, Pakdel, F, Flouriot, G, & Michel, D. (2012) Epigenetic memories: Structural marks or active circuits? *Cell Mol Life Sci* **69**, 2189–2203.

[95] To, T.-L & Maheshri, N. (2010) Noise can induce bimodality in positive transcriptional feedback loops without bistability. *Science* **327**, 1142–1145.

[96] Fitzgerald, J. B, Schoeberl, B, Nielsen, U. B, & Sorger, P. K. (2006) Systems biology and combination therapy in the quest for clinical efficacy. *Nat Chem Biol* **2**, 458–466.

[97] Piddock, L. J. V. (2006) Clinically relevant chromosomally encoded multidrug resistance efflux pumps in bacteria. *Clin Microbiol Rev* **19**, 382–402.

[98] Szakács, G, Paterson, J. K, Ludwig, J. A, Booth-Genthe, C, & Gottesman, M. M. (2006) Targeting multidrug resistance in cancer. *Nat Rev Drug Discov* **5**, 219–234.

[99] Wong, K, Ma, J, Rothnie, A, Biggin, P. C, & Kerr, I. D. (2014) Towards understanding promiscuity in multidrug efflux pumps. *Trends Biochem Sci* **39**, 8–16.

[100] Gulshan, K & Moye-Rowley, W. S. (2007) Multidrug resistance in fungi. *Eukaryot Cell* **6**, 1933–1942.

[101] Cannon, R. D, Lamping, E, Holmes, A. R, Niimi, K, Baret, P. V, Keniya, M. V, Tanabe, K, Niimi, M, Goffeau, A, & Monk, B. C. (2009) Efflux-mediated antifungal drug resistance. *Clin Microbiol Rev* **22**, 291–321.

[102] Yan, N. (2013) Structural advances for the major facilitator superfamily (MFS) transporters. *Trends Biochem Sci* **38**, 151–159.

[103] Gaur, M, Puri, N, Manoharlal, R, Rai, V, Mukhopadhayay, G, Choudhury, D, & Prasad, R. (2008) MFS transportome of the human pathogenic yeast Candida albicans. *BMC Genomics* **9**, 579.

[104] Coleman, J. J & Mylonakis, E. (2009) Efflux in fungi: la pièce de résistance. *PLoS Pathog* **5**, e1000486.

[105] Rees, D. C, Johnson, E, & Lewinson, O. (2009) ABC transporters: the power to change. *Nat Rev Mol Cell Biol* **10**, 218–227.

[106] Saraswathy, M & Gong, S. (2013) Different strategies to overcome multidrug resistance in cancer. *Biotechnol Adv* **31**, 1397–1407.

[107] Gillet, J.-P, Efferth, T, & Remacle, J. (2007) Chemotherapy-induced resistance by ATP-binding cassette transporter genes. *Biochim Biophys Acta* **1775**, 237–262.

[108] Lown, K. S, Mayo, R. R, Leichtman, A. B, Hsiao, H. L, Turgeon, D. K, Schmiedlin-Ren, P, Brown, M. B, Guo, W, Rossi, S. J, Benet, L. Z, & Watkins, P. B. (1997) Role of intestinal P-glycoprotein (mdr1) in interpatient variation in the oral bioavailability of cyclosporine. *Clin Pharmacol Ther* **62**, 248–260.

[109] Canaparo, R, Finnström, N, Serpe, L, Nordmark, A, Muntoni, E, Eandi, M, Rane, A, & Zara, G. P. (2007) Expression of CYP3A isoforms and P-glycoprotein in human stomach, jejunum and ileum. *Clin Exp Pharmacol Physiol* **34**, 1138–1144.

[110] Niimi, K, Maki, K, Ikeda, F, Holmes, A. R, Lamping, E, Niimi, M, Monk, B. C, & Cannon, R. D. (2006) Overexpression of Candida albicans CDR1, CDR2, or MDR1 does not produce significant changes in echinocandin susceptibility. *Antimicrob Agents Chemother* **50**, 1148–1155.

[111] Goffeau, A, Barrell, B. G, Bussey, H, Davis, R. W, Dujon, B, Feldmann, H, Galibert, F, Hoheisel, J. D, Jacq, C, Johnston, M, Louis, E. J, Mewes, H. W, Murakami, Y, Philippsen, P, Tettelin, H, & Oliver, S. G. (1996) Life with 6000 genes. *Science* **274**, 546–563–7.

[112] Barnett, J. A. (2000) A history of research on yeasts 2: Louis Pasteur and his contemporaries, 1850-1880. *Yeast* **16**, 755–771.

[113] Prasad, R & Goffeau, A. (2012) Yeast ATP-binding cassette transporters conferring multidrug resistance. *Annu Rev Microbiol* **66**, 39–63.

[114] Gupta, R. P, Kueppers, P, Schmitt, L, & Ernst, R. (2011) The multidrug transporter Pdr5: a molecular diode? *Biol Chem* **392**, 53–60.

[115] Ernst, R, Kueppers, P, Klein, C. M, Schwarzmueller, T, Kuchler, K, & Schmitt, L. (2008) A mutation of the H-loop selectively affects rhodamine transport by the yeast multidrug ABC transporter Pdr5. *Proc Natl Acad Sci USA* **105**, 5069–5074.

[116] Mamnun, Y. M, Schüller, C, & Kuchler, K. (2004) Expression regulation of the yeast PDR5 ATP-binding cassette (ABC) transporter suggests a role in cellular detoxification during the exponential growth phase. *FEBS Lett* **559**, 111–117.

[117] Kolaczkowski, M, van der Rest, M, Cybularz-Kolaczkowska, A, Soumillion, J. P, Konings, W. N, & Goffeau, A. (1996) Anticancer drugs, ionophoric peptides, and steroids as substrates of the yeast multidrug transporter Pdr5p. *J Biol Chem* **271**, 31543–31548.

[118] Kolaczkowski, M, Kolaczowska, A, Luczynski, J, Witek, S, & Goffeau, A. (1998) In vivo characterization of the drug resistance profile of the major ABC transporters and other components of the yeast pleiotropic drug resistance network. *Microb Drug Resist* **4**, 143–158.

[119] Prasad, R, Panwar, S. L, & Smriti. (2002) Drug resistance in yeasts–an emerging scenario. *Adv Microb Physiol* **46**, 155–201.

[120] Leppert, G, McDevitt, R, Falco, S. C, Van Dyk, T. K, Ficke, M. B, & Golin, J. (1990) Cloning by gene amplification of two loci conferring multiple drug resistance in Saccharomyces. *Genetics* **125**, 13–20.

[121] Katzmann, D. J, Burnett, P. E, Golin, J, Mahé, Y, & Moye-Rowley, W. S. (1994) Transcriptional control of the yeast PDR5 gene by the PDR3 gene product. *Mol Cell Biol* **14**, 4653–4661.

[122] Katzmann, D. J, Hallstrom, T. C, Mahé, Y, & Moye-Rowley, W. S. (1996) Multiple Pdr1p/Pdr3p binding sites are essential for normal expression of the ATP binding cassette transporter protein-encoding gene PDR5. *J Biol Chem* **271**, 23049–23054.

[123] Bauer, B. E, Wolfger, H, & Kuchler, K. (1999) Inventory and function of yeast ABC proteins: about sex, stress, pleiotropic drug and heavy metal resistance. *Biochim Biophys Acta* **1461**, 217–236.

[124] Gao, C, Wang, L, Milgrom, E, & Shen, W.-C. W. (2004) On the mechanism of constitutive Pdr1 activator-mediated PDR5 transcription in Saccharomyces cerevisiae: evidence for enhanced recruitment of coactivators and altered nucleosome structures. *J Biol Chem* **279**, 42677–42686.

[125] Voth, W. P, Takahata, S, Nishikawa, J. L, Metcalfe, B. M, Näär, A. M, & Stillman, D. J. (2014) A role for FACT in repopulation of nucleosomes at inducible genes. *PLoS ONE* **9**, e84092.

[126] Sanchez, A & Golding, I. (2013) Genetic determinants and cellular constraints in noisy gene expression. *Science* **342**, 1188–1193.

[127] Zenklusen, D, Larson, D. R, & Singer, R. H. (2008) Single-RNA counting reveals alternative modes of gene expression in yeast. *Nat Struct Mol Biol* **15**, 1263–1271.

[128] Hellauer, K, Akache, B, MacPherson, S, Sirard, E, & Turcotte, B. (2002) Zinc cluster protein Rdr1p is a transcriptional repressor of the PDR5 gene encoding a multidrug transporter. *J Biol Chem* **277**, 17671–17676.

[129] MacPherson, S, Larochelle, M, & Turcotte, B. (2006) A fungal family of transcriptional regulators: the zinc cluster proteins. *Microbiol Mol Biol Rev* **70**, 583–604.

[130] Wolfe, K. H & Shields, D. C. (1997) Molecular evidence for an ancient duplication of the entire yeast genome. *Nature* **387**, 708–713.

[131] Nourani, A, Papajova, D, Delahodde, A, Jacq, C, & Subik, J. (1997) Clustered amino acid substitutions in the yeast transcription regulator Pdr3p increase pleiotropic drug resistance and identify a new central regulatory domain. *Mol Gen Genet* **256**, 397–405.

[132] Schjerling, P & Holmberg, S. (1996) Comparative amino acid sequence analysis of the C6 zinc cluster family of transcriptional regulators. *Nucleic Acids Res* **24**, 4599–4607.

[133] Delaveau, T, Delahodde, A, Carvajal, E, Subik, J, & Jacq, C. (1994) PDR3, a new yeast regulatory gene, is homologous to PDR1 and controls the multidrug resistance phenomenon. *Mol Gen Genet* **244**, 501–511.

[134] Mamnun, Y. M, Pandjaitan, R, Mahé, Y, Delahodde, A, & Kuchler, K. (2002) The yeast zinc finger regulators Pdr1p and Pdr3p control pleiotropic drug resistance (PDR) as homo- and heterodimers in vivo. *Mol Microbiol* **46**, 1429–1440.

[135] Delahodde, A, Delaveau, T, & Jacq, C. (1995) Positive autoregulation of the yeast transcription factor Pdr3p, which is involved in control of drug resistance. *Mol Cell Biol* **15**, 4043–4051.

[136] Fardeau, V, Lelandais, G, Oldfield, A, Salin, H, Lemoine, S, Garcia, M, Tanty, V, Le Crom, S, Jacq, C, & Devaux, F. (2007) The central role of PDR1 in the foundation of yeast drug resistance. *J Biol Chem* **282**, 5063–5074.

[137] Ghaemmaghami, S, Huh, W.-K, Bower, K, Howson, R. W, Belle, A, Dephoure, N, O'Shea, E. K, & Weissman, J. S. (2003) Global analysis of protein expression in yeast. *Nature* **425**, 737–741.

[138] Thakur, J. K, Arthanari, H, Yang, F, Pan, S.-J, Fan, X, Breger, J, Frueh, D. P, Gulshan, K, Li, D. K, Mylonakis, E, Struhl, K, Moye-Rowley, W. S, Cormack, B. P, Wagner, G, & Näär, A. M. (2008) A nuclear receptor-like pathway regulating multidrug resistance in fungi. *Nature* **452**, 604–609.

[139] Näär, A. M & Thakur, J. K. (2009) Nuclear receptor-like transcription factors in fungi. *Genes Dev* **23**, 419–432.

[140] MacIsaac, K. D, Wang, T, Gordon, D. B, Gifford, D. K, Stormo, G. D, & Fraenkel, E. (2006) An improved map of conserved regulatory sites for Saccharomyces cerevisiae. *BMC Bioinformatics* **7**, –113.

[141] Salin, H, Fardeau, V, Piccini, E, Lelandais, G, Tanty, V, Lemoine, S, Jacq, C, & Devaux, F. (2008) Structure and properties of transcriptional networks driving selenite stress response in yeasts. *BMC Genomics* **9**, 333.

[142] Owsianik, G, Balzi l, L, & Ghislain, M. (2002) Control of 26S proteasome expression by transcription factors regulating multidrug resistance in Saccharomyces cerevisiae. *Mol Microbiol* **43**, 1295–1308.

[143] Moye-Rowley, W. S. (2003) Transcriptional control of multidrug resistance in the yeast Saccharomyces. *Prog Nucleic Acid Res Mol Biol* **73**, 251–279.

[144] Hallstrom, T. C & Moye-Rowley, W. S. (2000) Multiple signals from dysfunctional mitochondria activate the pleiotropic drug resistance pathway in Saccharomyces cerevisiae. *J Biol Chem* **275**, 37347–37356.

[145] Devaux, F, Carvajal, E, Moye-Rowley, S, & Jacq, C. (2002) Genome-wide studies on the nuclear PDR3-controlled response to mitochondrial dysfunction in yeast. *FEBS Lett* **515**, 25–28.

[146] Gietz, R. D & Schiestl, R. H. (2007) Frozen competent yeast cells that can be transformed with high efficiency using the LiAc/SS carrier DNA/PEG method. *Nat Protoc* **2**, 1–4.

[147] Shao, Z, Zhao, H, & Zhao, H. (2009) DNA assembler, an in vivo genetic method for rapid construction of biochemical pathways. *Nucleic Acids Res* **37**, e16.

[148] Sheff, M. A & Thorn, K. S. (2004) Optimized cassettes for fluorescent protein tagging in Saccharomyces cerevisiae. *Yeast* **21**, 661–670.

[149] Huh, W.-K, Falvo, J. V, Gerke, L. C, Carroll, A. S, Howson, R. W, Weissman, J. S, & O'Shea, E. K. (2003) Global analysis of protein localization in budding yeast. *Nature* **425**, 686–691.

[150] Schneider-Poetsch, T, Ju, J, Eyler, D. E, Dang, Y, Bhat, S, Merrick, W. C, Green, R, Shen, B, & Liu, J. O. (2010) Inhibition of eukaryotic translation elongation by cycloheximide and lactimidomycin. *Nat Chem Biol* **6**, 209–217.

[151] Saoudi, Y, Fotedar, R, Abrieu, A, Dorée, M, Wehland, J, Margolis, R. L, & Job, D. (1998) Stepwise reconstitution of interphase microtubule dynamics in permeabilized cells and comparison to dynamic mechanisms in intact cells. *J Cell Biol* **142**, 1519–1532.

[152] Xu, K, Schwarz, P. M, & Ludue a, R. F. (2002) Interaction of nocodazole with tubulin isotypes. *Drug Dev Res* **55**, 91–96.

[153] Hillenmeyer, M. E, Fung, E, Wildenhain, J, Pierce, S. E, Hoon, S, Lee, W, Proctor, M, St Onge, R. P, Tyers, M, Koller, D, Altman, R. B, Davis, R. W, Nislow, C, & Giaever, G. (2008) The chemical genomic portrait of yeast: uncovering a phenotype for all genes. *Science* **320**, 362–365.

[154] Suzuki, G, Shimazu, N, & Tanaka, M. (2012) A yeast prion, Mod5, promotes acquired drug resistance and cell survival under environmental stress. *Science* **336**, 355–359.

[155] Johnson, S, Nguyen, V, & Coder, D. (2013) in *Current protocols in cytometry*. (John Wiley & Sons, Inc.), p. Unit 9.2.

[156] Lehner, B. (2008) Selection to minimise noise in living systems and its implications for the evolution of gene expression. *Mol Syst Biol* **4**, 170.

[157] Wang, Z & Zhang, J. (2011) Impact of gene expression noise on organismal fitness and the efficacy of natural selection. *Proc Natl Acad Sci USA* **108**, E67–76.

[158] Hazelwood, L. A, Walsh, M. C, Pronk, J. T, & Daran, J.-M. (2010) Involvement of vacuolar sequestration and active transport in tolerance of Saccharomyces cerevisiae to hop iso-alpha-acids. *Appl Environ Microb* **76**, 318–328.

[159] Plemper, R. K, Egner, R, Kuchler, K, & Wolf, D. H. (1998) Endoplasmic reticulum degradation of a mutated ATP-binding cassette transporter Pdr5 proceeds in a concerted action of Sec61 and the proteasome. *J Biol Chem* **273**, 32848–32856.

[160] Rockwell, N. C, Wolfger, H, Kuchler, K, & Thorner, J. (2009) ABC transporter Pdr10 regulates the membrane microenvironment of Pdr12 in Saccharomyces cerevisiae. *J Membr Biol* **229**, 27–52.

[161] Yibmantasiri, P, Bircham, P. W, Maass, D. R, Bellows, D. S, & Atkinson, P. H. (2014) Networks of genes modulating the pleiotropic drug response in Saccharomyces cerevisiae. *Mol Biosyst* **10**, 128–137.

[162] De Deken, R. H. (1966) The Crabtree effect: a regulatory system in yeast. *J Gen Microbiol* **44**, 149–156.

[163] Dimitrov, L. N, Brem, R. B, Kruglyak, L, & Gottschling, D. E. (2009) Polymorphisms in multiple genes contribute to the spontaneous mitochondrial genome instability of Saccharomyces cerevisiae S288C strains. *Genetics* **183**, 365–383.

[164] Warringer, J, Zörgö, E, Cubillos, F. A, Zia, A, Gjuvsland, A, Simpson, J. T, Forsmark, A, Durbin, R, Omholt, S. W, Louis, E. J, Liti, G, Moses, A, & Blomberg, A. (2011) Trait variation in yeast is defined by population history. *PLoS Genet* **7**, e1002111.

[165] Belle, A, Tanay, A, Bitincka, L, Shamir, R, & O'Shea, E. K. (2006) Quantification of protein half-lives in the budding yeast proteome. *Proc Natl Acad Sci USA* **103**, 13004–13009.

[166] Tomala, K & Korona, R. (2013) Evaluating the fitness cost of protein expression in Saccharomyces cerevisiae. *Genome Biol Evol* **5**, 2051–2060.

[167] Balzi, E, Chen, W, Ulaszewski, S, Capieaux, E, & Goffeau, A. (1987) The multidrug resistance gene PDR1 from Saccharomyces cerevisiae. *J Biol Chem* **262**, 16871–16879.

[168] Paul, S & Moye-Rowley, W. S. (2014) Multidrug resistance in fungi: regulation of transporter-encoding gene expression. *Front Physiol* **5**, 143.

[169] Kolaczkowska, A, Kolaczkowski, M, Delahodde, A, & Goffeau, A. (2002) Functional dissection of Pdr1p, a regulator of multidrug resistance in Saccharomyces cerevisiae. *Mol Genet Genomics* **267**, 96–106.

[170] Poch, O. (1997) Conservation of a putative inhibitory domain in the GAL4 family members. *Gene* **184**, 229–235.

[171] Simonics, T, Kozovska, Z, Michalkova-Papajova, D, Delahodde, A, Jacq, C, & Subik, J. (2000) Isolation and molecular characterization of the carboxy-terminal pdr3 mutants in Saccharomyces cerevisiae. *Curr Genet* **38**, 248–255.

[172] Soontorngun, N. (2008) Ph.D. thesis (McGill University, Montreal).